博士論文 (要約)

Studies on the estimation of water temperature experienced during the larval stage of Pacific bluefin tuna *Thunnus orientalis* using SIMS oxygen isotope analysis of otoliths

(SIMSによる耳石酸素安定同位体比分析を用いた
クロマグロ仔魚期の経験水温の推定に関する研究)

Yulina Hane

羽根 由里奈

Acknowledgement

My sincere gratitude goes first to my supervisor Prof. Shingo Kimura, who guided me throughout the entire course of my graduate education since I have become a member of his laboratory in 2013. His expertise and enthusiasm in the field of biological oceanography gave me an inspiration to pursue a career in science and taught me what it is like to be a researcher. My research journey would not have been possible without his valuable advice, expertise, and supervision.

I would also like to thank Prof. Yusuke Yokoyama whose expertise in interdisciplinary academic topics broadened my perspectives and pushed me think and explore out the box. I would also like to thank him for reviewing my thesis and providing valuable suggestions. My heartfelt gratitude also goes to Dr. Takayuki Ushikubo of the Kochi Core Center of Japan Agency for Marine-Earth Science and Technology and Assoc. Prof. Toyoho Ishimura of Kyoto University who kindly provided me necessary technical support and constructive advice whenever I encountered difficulties in carrying out my research. I would also like to extend my appreciation to Dr. Yosuke Miyairi and Dr. Nobuhiro Ogawa for the stimulating discussions with challenging questions which incented me to think beyond the scope of my research. I am also grateful to Dr. Yoichi Miyake of the National Research Institute of Fisheries and Environment of Inland Sea for his critical feedback on my research that always navigated me into the right direction. I would also like to thank Prof. Shigeaki Kojima, Assoc. Prof. Kosei Komatsu, and Assoc. Prof. Shigeyoshi Otosaka for their critical review on my doctoral dissertation and insightful and extremely helpful comments that improved the quality of the thesis. My warm appreciation also goes to Dr. Shengle Yin, Dr. Kuan-Mei Hsiung, and members of Biological Oceanography Group in the Atmosphere and Ocean Research Institute who supported me with great care and love and helped me get through hard times and countless sleepless nights. I would also like to thank Dr. Kozue Nishida of University of Tsukuba and Mr. Tomoya Aono for their technical support and critical suggestions on the design of the experiment.

Last but not least, I would like to give my warmest thanks to my family for always being there for me and supportive and encouraging me whenever I had difficulties in the course of completing the doctoral degree. I could not thank enough for the love and support that you have given me.

CHAPTER 1

Chapter 1 cannot be viewed because the contents will be published in an academic journal.

CHAPTER 2

Chapter 2 cannot be viewed because the contents will be published in an academic journal.

CHAPTER 3

Temperature reconstruction using otolith $\delta^{18}O$

3.1. Introduction

Ocean warming causes significant impacts on marine species and ecosystems, including high mortality, distribution shifts, and loss of spawning and nursery habitats (Perry et al., 2005, Kimura et al., 2010, Muhling et al., 2011, 2015). Species that spawn seasonally in relatively limited areas are particularly vulnerable to increasing water temperature, as their optimum range in spawning temperatures tends to be restricted. Pacific bluefin tuna is a highly migratory species that spawns in waters near the Nansei Islands in the western North Pacific from May to June and in the Sea of Japan from July to August (Yonemori 1989, Ohshimo et al., 2017). Adult fish in the western North Pacific spawn at temperatures between 26 and 29°C, whereas those in the Sea of Japan initiate spawning at temperatures greater than 20°C (Chen et al., 2006, Tanaka 2011, Suzuki et al., 2014, Okochi et al., 2016). In the laboratory, the growth rate and survival of Pacific bluefin tuna larvae significantly decrease when temperatures exceed 29°C (Kimura et al., 2007). In fact, projected temperature in the current spawning sites is expected to increase by more than 3°C by 2100 under the most extreme IPCC climate-warming scenario (IPCC 2007) and become unsuitable for Pacific bluefin tuna to spawn (Kimura et al., 2010). As bluefin larvae are particularly vulnerable to thermal stress, warming sea temperatures are likely to cause significant impacts on their early growth and survival. However, the effects of ongoing climate change on the early life stages of Pacific bluefin tuna are poorly understood due to a lack of empirical evidence and methods to study such effects.

Oxygen isotope ratios ($\delta^{18}O$) in otoliths, biogenic calcium carbonate (aragonite) found in the inner ear of teleost fish (ray-finned bony fish), has been widely used as a natural tag to reconstruct water temperatures and salinity conditions experienced by fish (Thorrold et al., 1997, Campana 1999, Jones

& Campana 2009). Such reconstructions of past environment are possible because otoliths generally develop at or close to the isotope equilibrium with ambient water, and many studies have demonstrated the temperature-dependency of otolith $\delta^{18}O$ for various fish species under laboratory conditions (Kalish 1991, Thorrold et al., 1997, Høie et al., 2004, Kitagawa et al., 2013). Existing methods of temperature reconstruction for fish mostly rely on $\delta^{18}O_{otolith}$ measurements by conventional isotope ratio mass spectrometer (IRMS), which often involves a milling process to obtain a relatively large amount of otolith powder for analysis (usually > a few tens of micrograms with a minimum weight requirement of 15 μg). Ambient water temperatures have previously been reconstructed using IRMS for sockeye salmon *Oncorhynchus nerka* (Zazzo et al., 2006), alewife *Alosa pseudoharengus* (Dufour et al., 2008), Atlantic cod *Gadus morhua* (Jones & Campana 2009, Leesen et al., 2020), turbot *Scophthalmus maximus* (Imsland et al., 2014), and chub mackerel *Scomber japonicus* (Higuchi et al., 2019), most of which have a monthly to annual resolution depending on the otolith size. The limited temporal resolution due to the sample mass requirement of the IRMS is inevitable and makes it particularly difficult when analyzing the otolith core and edge.

The recent developments in secondary ion mass spectrometry (SIMS) $\delta^{18}O$ analysis of otoliths have enabled a high-resolution reconstruction of migration and life history characteristics of marine species (Hanson et al., 2010, Matta et al., 2013, Shiao et al., 2014, Helser et al., 2018a, Shirai et al., 2018, Willmes et al., 2019). Unlike conventional IRMS, SIMS is capable of determining isotopic composition within a spatial resolution of 5–15 μm, which allows sub-annual, seasonal, and even weekly or much shorter timescale analyses with high accuracy and precision (Valley & Kita 2009, Kita et al., 2009). While a recent study (Sakamoto et al., 2019) reconstructed migration histories of an individual Japanese sardine *Sardinops melanostictus* with 10–30 days resolution (20–30 days around the core regions and 10–15 days toward the edge) using microvolume isotope analysis measured by continuous-flow IRMS (CF-IRMS), SIMS provides even finer temporal resolution, particularly for the otolith core and edge. High-resolution reconstruction of experienced temperatures using SIMS

$\delta^{18}O_{otolith}$ has important utility to investigate the early life history of fish that may be affected by increasing water temperature associated with climate change.

In this chapter, we aim to develop a method to reconstruct ambient water temperatures experienced during the larval period of an individual fish using SIMS $\delta^{18}O_{otolith}$ analysis. $\delta^{18}O_{otolith}$ of five adult Pacific bluefin tuna are measured from the otolith core to edge by SIMS, and the measured SIMS $\delta^{18}O_{otolith}$ values were compared to those measured by CF-IRMS. Water temperatures are then estimated using a temperature-dependent oxygen isotope fractionation equation for Pacific bluefin tuna larvae that has been already established in the previous study (Kitagawa et al., 2013). The temperature reconstruction technique presented here allows for a high-resolution investigation of the early life history of fish and provides a more thorough understanding of the characteristics of survivors and thermal environment that may constrain their early growth and survival.

3.2. Materials and Methods

3.2.1. Sample collection and sample preparation

Otoliths were collected from the defrosted heads of Pacific bluefin tuna caught mostly by longline fishing gear in waters around Japan from 2017 to 2018 (Fig. 3-1). In total, otoliths from 119 bluefin tuna (sub-adult and adult) were collected. As data on fish weight was only available, the fork length of fish was estimated using a weight–length relationship established by Kai (2007). The otolith weight (length) and estimated weight (fork length) of the fish collected in this study and those of young-of-the-year fish (Suzuki, 2019) were measured, and their relationship with fish weight and fork length was determined, respectively (Figs. 3-2, 3-3, 3-4).

Age of the fish was determined according to the age reading protocol that has been already developed for Pacific bluefin tuna (Shimose & Ishihara, 2015) (Fig. 3-5). The relationship between

otolith weight (length) and fish weight for sub-adult and adult, young-of-the-year fish, and those combined is shown in Fig. 3-2a (b), Fig. 3-3a (b), and Fig. 3-4a (b), respectively.

Five adult fish samples were randomly selected and one of paired otoliths from each individual was used for SIMS $\delta^{18}O$ analysis. Catch location, date of catch, and biological information of bluefin tuna samples are shown in Fig. 3-6 and Table 3. Otoliths were cleaned and rinsed with double deionized water (Milli-Q water) to remove any remaining muscle tissues, air-dried in a clean environment, and stored in microtubes for later analyses. For CF-IRMS $\delta^{18}O$ analysis, the three otolith sections that were analyzed by SIMS were used.

For the preparation of otolith samples for SIMS $\delta^{18}O$ analysis, we used the sample preparation protocol for a single otolith thin section that has been previously developed in Chapter 2. A detailed sample preparation protocol can be found in Fig. 2-1. Briefly, an otolith was mounted on a microscope slide with thermoplastic cement perpendicular to the sagittal plane with its sulcus side facing down. The otolith core was observed under an inverted microscope (IX-71, Olympus) and straight lines were drawn on the glass slide at 250 to 270 μm on each side of the otolith core using waterproof ink and a comic pen. An otolith thin section was cut out together with the glass slide along the drawn lines with an automatic low-speed precision cutter (IsoMet 5000, Buehler) equipped with a 0.3 mm thick diamond blade (IsoMet 15LC, Buehler). The sectioned otolith was then removed from a strip of glass by rinsing it with acetone and was allowed to air-dry in a laminar flow hood. The sectioned otolith was fixed in the center of a 2.54 cm silicon mold and embedded in epoxy (EpoxyCure 2 Resin, Buehler) along with a UWC-3 standard, that was placed right above the otolith. It was then kept at room temperature for 24 h to cure the resin. The epoxy disk containing an otolith thin section and a piece of standard material was ground with a grinding machine equipped with 70 and 13 μm diamond cup wheels (Discoplan-TS, Struers) until the distance from the otolith surface to the core reached 15 to 20 μm. It was then successively polished using 6, 3, and 1 μm diamond pastes on a fine grinding disc (MD-Largo, Struers) to expose the core on a flat mirror-finished surface.

Before analysis, the samples were cleaned in an ultrasonic cleaner and dried in a vacuum oven at 40 °C for 2 h. They were then sputter-coated with ~60 nm gold.

3.2.2. SIMS $\delta^{18}O$ analysis

Otolith oxygen isotope ratios were measured *in situ* using a CAMECA IMS 1280-HR large radius, multi-collector ion microprobe (SIMS) at the Kochi Institute for Core Sample Research, Japan Agency for Marine-Earth Science and Technology (JAMSTEC). Five otolith thin sections were prepared for SIMS $\delta^{18}O_{otolith}$ analyses using the sample preparation protocol developed in the present study (Fig. 2-1). The $\delta^{18}O_{otolith}$ values were measured from otolith core to edge along the growth axis for each otolith sample (Fig. 3-7).

The SIMS analytical conditions that were used for $\delta^{18}O_{otolith}$ measurements in this study are described in detail in Kita et al., (2009). The sample surface was sputtered by a 20 kV accelerated $^{133}Cs^{+}$ primary ion beam of 1.5–1.8 nA focused to a diameter of 10 to 15 μm, resulting in a pit of ~1 μm depth (Fig. 3-7b). The secondary ions ($^{16}O^{-}$, $^{18}O^{-}$, and $^{16}OH^{-}$) were accelerated at 10 kV and detected simultaneously by three Faraday cup detectors. Since hydrogen is present in the SIMS chamber even under ultra-high vacuum conditions, measured $^{16}OH^{-}/^{16}O^{-}$ ratios were background-corrected by subtracting the average $^{16}OH^{-}/^{16}O^{-}$ ratio of the UWC-3 standard (nominally anhydrous minerals) bracketing analyses from the $^{16}OH^{-}/^{16}O^{-}$ ratio of $\delta^{18}O_{otolith}$ measurements. The background-corrected $^{16}OH^{-}/^{16}O^{-}$ ratios served as a proxy for the relative hydrogen content contained in otolith samples. Each analysis took ~3 min, consisting of pre-sputtering (10 s), automatic centering of the secondary ion beam (90 s), and the isotopic measurements with 20 analytical cycles (40 s). The count rates for $^{16}O^{-}$ and $^{18}O^{-}$ were 1.7–2.5 × 10^{9} and 3.5–5.1 × 10^{6} counts per second (cps), respectively.

For accurate calibration of SIMS $\delta^{18}O$ measurements in biogenic carbonate samples, a homogeneous biocarbonate standard with a matched-matrix is needed. The UWC-3 standard is a

chemically and isotopically homogeneous calcite standard which has a similar chemical composition as otoliths (aragonite), and thus all $\delta^{18}O_{otolith}$ measurements were normalized with this standard in our study (Kozdon et al., 2009). Every 10 to 15 unknown sample measurements were bracketed by 10 analyses of a UWC-3 calcite standard (5 analyses before and after each group of unknown samples) to calculate the spot-to-spot precision of sample analyses and to correct for instrumental mass fractionation. The precision of sample analyses for all 5 otolith thin sections was ±0.3 to ±0.6‰ (2 standard deviations).

After analysis, each spot was observed on scanning electron microscope (SEM) images taken with an electron probe micro analyzer (JXA-8230, JEOL) to check for any cracks and inclusions that might bias the resulting $\delta^{18}O$ values (e.g. Weidel et al., 2007). No spots had such surface irregularities. In addition, the secondary ion yield ($^{16}O^-$, cps/nA) relative to the mean of the UWC-3 standard bracketing analyses were used to assess the quality of each spot measurement and check for any extreme outliers. Raw SIMS $\delta^{18}O$ measurements are presented in Table S1.

For comparison purposes, all $\delta^{18}O_{otolith}$ values were converted from VSMOW to VPDB by using the latest published conversion equation ($\delta^{18}O_{VSMOW} = 1.03092 * \delta^{18}O_{VPDB} + 30.92$, Brand et al., 2014, Kim et al., 2015).

3.2.3. Microvolume $\delta^{18}O$ analysis by CF-IRMS

Microvolume CF-IRMS $\delta^{18}O$ analysis was conducted to compare $\delta^{18}O_{otolith}$ values measured by SIMS and CF-IRMS. Three otolith thin sections that were analyzed by SIMS were used for microvolume CF-IRMS $\delta^{18}O$ analysis. $\delta^{18}O$ analyses were performed with an IsoPrime100 isotope ratio mass spectrometer (Isoprime Ltd, Cheadle Hulme, UK) equipped with a customized continuous-flow gas preparation system (MICAL3c) at National Institute of Technology, Ibaraki College, Japan. This system can measure isotope ratios of calcium carbonate samples with a minimum sample mass

of 0.2 μg (about 1/100 of the sample mass required for commercially available IRMS systems) with high precision and accuracy (Ishimura et al., 2004, 2008). By micromilling the otolith material deposited during the same growth period that is being analyzed by SIMS, it is possible to compare average SIMS and CF-IRMS $\delta^{18}O_{otolith}$ values.

A high precision micromilling system (Geomill326) was used for milling the specific regions of otolith samples. This system comprised a carbide bur fixed over an XYZ sample stage, a high-resolution camera, and a computerized image analyzer. An otolith image with marks indicating the target milling areas was imported into the system and milling paths were configured on the computer. The target milling areas were set in the otolith region where the measured SIMS $\delta^{18}O_{otolith}$ values were stable, and they covered roughly 3–4 SIMS beam spots (Fig. 3-8). First, an unwanted area right next to the target milling path was milled and removed from otolith to avoid cross-contamination. The removed otolith powders were also collected and used for analysis as supplementary samples to increase the dataset. For each otolith sample, two to three target paths were milled along the growth rings to obtain powder samples. The milled paths resulted 15 to 80 μm wide, 250 to 350 μm long, and 60 to 90 μm deep.

The life stages of the corresponding milled paths were estimated based on the distance from otolith core and the location of the annual growth increments. Each path corresponded to either the juvenile (a few months old), immature (about 5 months old to age 1+), or sub-adult stage (age 2–3). The non-parametric Kruskal-Wallis test was used to determine the statistical difference in resulting offset values between SIMS and CF-IRMS among different life stages.

The amount of powder produced from each path was 0.9 to 3.5 μg. The milled powder was carefully collected and placed on to a small piece of glass using a needle under a microscope, and then put into the bottom of a reaction tube. The aragonite powder was then reacted with phosphoric acid at 25°C, and the evolved CO_2 was purified in a stainless vacuum line. After further purification

using a helium-purged purification line, the purified CO_2 was introduced into the mass spectrometer. Samples that weighed more than 2.0 μg were analyzed twice. The results are reported in standard δ notation (‰) relative to Vienna Pee Dee Belemnite (VPDB). We measured a lab standard CO_2 gas for the determination of the analytical precision of pure CO_2 gas ($\delta^{13}C_{VPDB}$ = −1.56‰ and $\delta^{18}O_{VPDB}$ = −4.42‰, Nishida & Ishimura 2017) three or more times every day. The analytical precision was better than ± 0.1‰ (± 1SD) for the entire analysis.

To compare the difference between SIMS and CF-IRMS values, the average SIMS $\delta^{18}O_{otolith}$ values were calculated by averaging the SIMS spot measurements adjacent to or within each milling path and then compared to CF-IRMS $\delta^{18}O_{otolith}$ value. A linear regression analysis was performed to determine the correlation between values measured by the two methods. In addition, the Wilcoxon signed rank test was applied to test the statistical difference between the average SIMS and CF-IRMS $\delta^{18}O_{otolith}$ values, and the Tukey's test was used to detect outliers. All statistical analyses were performed using the R software (version 3.3.2).

3.2.4. Temperature reconstruction for larval stages of adult bluefin tuna

Ambient water temperatures experienced during the larval stages of adult bluefin were estimated using SIMS $\delta^{18}O_{otolith}$ of otolith core region. The daily growth increments were counted around the core region on the SEM images. The SIMS spot measurements that were made within 20 days post hatch (DPH) were used for the temperature estimation as the larval period of bluefin tuna lasts for approximately 20 days. For an accurate estimation of ambient water temperatures, a species-specific fractionation equation and $\delta^{18}O_{seawater}$ are needed. To reconstruct ambient temperatures, we used the oxygen isotope fractionation equation for Pacific bluefin tuna larvae proposed by Kitagawa et al. (2013):

$$\delta^{18}O_{otolith\ (VPDB)} - \delta^{18}O_{water\ (VPDB)} = 5.193 - 0.270 \times T \quad (3\text{-}1)$$

where $\delta^{18}O_{water}$ is the $\delta^{18}O$ value of ambient water, and T is the water temperature in °C. For $\delta^{18}O_{water}$ in the equation, we applied the $\delta^{18}O$ value of +0.22‰ (VSMOW) which is the average $\delta^{18}O_{water}$ of the main spawning ground around the Nansei Islands (123.56-131.00°E, 24.04-26.09°N) in May to June from 2008 to 2010 (Uozato 2011). The $\delta^{18}O_{seawater}$ value was corrected on the VPDB scale by simply subtracting 0.27‰ (Hut 1987). The mean temperatures were calculated for the samples that had multiple $\delta^{18}O_{otolith}$ measurements made around the core regions. Although the focus was on the reconstruction of ambient water temperatures experienced during the larval period of the fish, the lifetime temperature history was estimated to evaluate how well $\delta^{18}O_{otolith}$ records ambient water temperatures in the older stages of Pacific bluefin tuna.

3.3. Results

3.3.1. Comparison of SIMS and CF-IRMS $\delta^{18}O_{otolith}$ measurements

In total, 22 paths were milled by a micromilling system and $\delta^{18}O_{otolith}$ of collected powders from each milled path was measured by CF-IRMS. After carefully examining the accuracy of how well each milled path captured the same growth zone as the SIMS spots, 18 samples, including 9 main samples and 9 supplementary samples, were selected to assess the difference between SIMS and CF-IRMS $\delta^{18}O_{otolith}$ values. The average values of multiple CF-IRMS measurements were used when the milling accuracy of a single milling path was low (See Appendix 2 for a complete list of data). The precision of $\delta^{18}O_{otolith}$ values measured by CF-IRMS was better than that of SIMS.

The $\delta^{18}O_{otolith}$ values measured by CF-IRMS were significantly higher than those measured by SIMS (Fig. 3-9, Wilcoxon signed-rank test, $p < 0.001$) except for two measurements in which the CF-IRMS value was 0.12‰ and 0.47‰ lower than the average SIMS value, respectively. We considered

the CF-IRMS $\delta^{18}O_{otolith}$ measurement that resulted 0.47‰ lower than the average SIMS $\delta^{18}O_{otolith}$ value as an outlier based on the Tukey's outlier detection method. This measurement was taken from a relatively large area of the otolith deposited during the second to third years of life, where the interannual variation in water temperature is expected. It is likely that this temperature variation was not well reflected in the average SIMS value since only 3 spot measurements were averaged over more than a half-year period. Therefore, this measurement was excluded for calculating a linear regression curve and the average SIMS–CF-IRMS difference.

There was a significant positive correlation between SIMS and CF-IRMS $\delta^{18}O_{otolith}$ values (r^2 = 0.79, $p < 0.001$) with a slope of 1.1408 and an intercept of 0.0704. The slope is 1 within the 95% confidence interval (lower limit = 0.82, upper limit = 1.46) with a high correlation coefficient (r^2 = 0.78), and thus a linear regression with a slope of 1 was fitted to the data to calculate the y-intercept, which is the average difference (Fig. 3-10). The average offset between SIMS and CF-IRMS $\delta^{18}O_{otolith}$ values was 0.41‰, with SIMS yielding lower values. The SIMS–CF-IRMS $\delta^{18}O_{otolith}$ correction equation for Pacific bluefin tuna can be expressed as:

$$\text{SIMS } \delta^{18}O_{otolith\ (VPDB)} = \text{CF-IRMS } \delta^{18}O_{otolith\ (VPDB)} - 0.41 \quad (3\text{-}2)$$

No significant difference was observed between $\delta^{18}O_{otolith}$ measurements at different life stages (Kruskal-Wallis test, $p = 0.29$), and thus the consistent application of this offset correction equation to all SIMS measurements was considered appropriate.

3.3.2. Seasonal variations in SIMS $\delta^{18}O_{otolith}$ profiles

In total, 259 $\delta^{18}O_{otolith}$ measurements were made on the otoliths of five Pacific bluefin tuna by SIMS (Table 3). The total number of spots measured per otolith was 42 to 78 (two life-history transect

lines were analyzed for T64R). The length of each transect ranged between 2.5 mm and 2.8 mm with a spot-to-spot distance ranging from 16 μm to 153 μm around the core region, and 26 μm to 337 μm toward the edge. The spatial resolution around the core region in one of the samples was more than 10 times higher compared to the conventional IRMS method previously used for Pacific bluefin tuna otoliths (Shiao et al., 2010). The temporal resolution of SIMS spots was 3–5 days near the core region and roughly a few weeks to a month on the outer edge depending on the age of fish.

The offset-corrected SIMS $\delta^{18}O_{otolith}$ values for 5 Pacific bluefin tuna samples are plotted in Fig. 3-11 (see left y-axis). High-resolution $\delta^{18}O_{otolith}$ profiles of all otolith samples showed distinct seasonal variations with an increasing trend from the otolith core to about 1250 μm. The average $\delta^{18}O_{otolith}$ values from the core to about 750 μm ranged between −3.1 to −2.5‰ (VPDB), and sharply increased toward the first annual increment (opaque zone), peaking at −1.3 to −0.4‰. After the increase, the $\delta^{18}O_{otolith}$ values decreased, showing a cyclical pattern toward the edge fluctuating mostly between −2.5 to −1.5‰ (VPDB). The $\delta^{18}O_{otolith}$ of the core regions corresponding to the larval stages (10 to 20 DPH) of bluefin tuna ranged between −3.1 to −1.9‰ (VPDB).

The background-corrected $^{16}OH^{-}/^{16}O^{-}$ ratios measured for the five otoliths ranged between 0.017 and 0.031 and had a general inverse relationship with the SIMS $\delta^{18}O_{otolith}$ values (there is no impact of individual differences on this relationship) (Fig. 3-12a). This indicates that the relative hydrogen content in the otolith increases with lower SIMS $\delta^{18}O_{otolith}$ values. Overall, higher $^{16}OH^{-}/^{16}O^{-}$ ratios resulted in larger SIMS–CF-IRMS $\delta^{18}O_{otolith}$ differences (Fig. 3-12b), which is consistent with the inverse trend seen in Fig. 3-12a.

3.3.3. Estimation of temperature experienced during larval period

Core-to-edge water temperature profiles of all samples are shown in Fig. 3-11 (see right y-axis). The estimated temperatures experienced during the larval stages ranged between 26.7°C to 30.7°C

among the individuals (T64R: 30.7 ± 1.3°C [~20 DPH], T75R: 27.9 ± 1.0°C [~10 DPH], T104L: 26.7 ± 1.0°C [~12 DPH], T118R: 28.9 ± 0.9°C [~12 DPH], T131R: 28.4 ± 1.4°C [~12 DPH]). After the year 0, temperature raged mostly between 24 and 30°C, and never reached 35°C.

3.4. Discussion

An increasing number of experimental and modeling studies have shown significant impacts of projected climate change on the early growth and survival of various fish species (Kimura et al 2007, Pankhurst & Munday 2011, Moyano et al., 2017). Generally, fish larvae are more sensitive to temperature variations than juveniles and adults as they have narrower thermal tolerance ranges (Pörtner & Peck 2010, Moyano et al., 2017), making them particularly vulnerable to climate change. However, the effects of ongoing climate change-driven ocean warming on the early life history of fish remain largely unexplored for many species, mostly due to difficulties in monitoring long-term responses to climatic stressors. Thus, the advancement of techniques that can quantitatively estimate past environments actually experienced by fish during key phases of the life cycle is essential to fill this knowledge gap. In this study, a high-resolution temperature reconstruction technique using SIMS $\delta^{18}O_{otolith}$ analysis was developed and applied to Pacific bluefin tuna, a species of great economic importance, whose early larval growth and survival may be constrained by climate change.

The 0.41‰ offset observed between SIMS and CF-IRMS $\delta^{18}O_{otolith}$ values for bluefin tuna otoliths is most likely due to incomplete correction for “matrix effects” by SIMS methods. Matrix effects refer to an instrumental mass fractionation caused by different chemical compositions and structures between given samples and standard materials, which shifts measured values (Eiler et al., 1997, Riciputi et al., 1998, Śliwiński et al., 2016, 2017, Wycech 2018). Otoliths contain a small amount of organic proteins, namely otolith matrix protein-1 and Otolin-1 (Murayama et al., 2000, 2002). The presence of these proteins in the otolith would be responsible for a subtle change in instrumental mass

fractionation, which results in lower SIMS $\delta^{18}O_{otolith}$ values relative to those measured by CF-IRMS and higher $^{16}OH^-$ ion yields compared to that of the calcite standard. The general inverse relationship between $^{16}OH^-/^{16}O^-$ ratios and SIMS $\delta^{18}O_{otolith}$ values (Fig. 3-12a) may be the result of the incorporation of more proteins into the otolith matrix which is thought to relate to fast growth in summer (or less proteins in winter due to slow growth). Water content (OH^-) of the otoliths, if any, is also responsible for the lower $\delta^{18}O_{otolith}$ values. These organic proteins and water content bias SIMS $\delta^{18}O_{otolith}$ values because they are measured together with calcium carbonates, whereas they do not affect CF-IRMS $\delta^{18}O_{otolith}$ values since these proteins do not react with phosphoric acid at 25°C that is used in a digestion process to generate CO_2 gas. Furthermore, the systematic difference in isotopic fractionations caused by sputtering different crystalline structures (the biogenic aragonite samples and calcite standard) may contribute to the observed offset (Linzmeier et al., 2016). Although matrix effects are likely the primary cause of the SIMS–CF-IRMS difference, other potential factors (e.g. milling and roasting effects) may influence the measurement results of SIMS and CF-IRMS. The effects of roasting and other factors are discussed in detail in Wycech et al. (2018) which investigated the $\delta^{18}O$ difference between SIMS and IRMS using foraminiferal shells.

The offset of 0.41‰ found in this study is within the range of offset values previously reported for otolith of other fish species and biocarbonate samples. Orland et al. (2015) has reported that there is a consistent sample-dependent offset in $\delta^{18}O$ typically less than 1.0‰, but it can go up to 1.8‰ depending on different sample matrices including biocarbonates and speleothems. Matta et al. (2013) used roasting to remove organic materials and observed an offset of about 1‰ in SIMS $\delta^{18}O$ values between roasted and unroasted otoliths of a yellowfin sole *Limanda aspera.* Helser et al. (2018b) also observed a 0.5‰ offset between SIMS and CF-IRMS $\delta^{18}O_{otolith}$ measurements in otoliths of Pacific cod *Gadus macrocephalus.* The temperature estimation without the correction of the 0.41‰ offset using SIMS $\delta^{18}O_{otolith}$ values of Pacific bluefin tuna would cause a bias of 1.5°C in the estimates, resulting in some unrealistically high temperature estimates (i.e. >34°C). While it is unknown to what

extent organic proteins and water content contribute to an overall offset, it is necessary to determine these offsets between SIMS versus IRMS when estimating ambient water temperatures from SIMS $\delta^{18}O_{otolith}$ values for different species.

The SIMS analyses performed on five otolith samples of Pacific bluefin tuna revealed fine-scale $\delta^{18}O_{otolith}$ profiles from the core to the edge with clear seasonal variations (Fig. 3-11). As water temperature and $\delta^{18}O_{otolith}$ are negatively correlated (Devereux 1967, Høie et al., 2004, Thorrold et al., 1997), the initial increase of the $\delta^{18}O_{otolith}$ values observed toward the first annual increment (opaque zone) for all otolith samples indicates that Pacific bluefin tuna experienced a decreasing water temperature. Age-0 juveniles predominantly inhibit in the surface mixed layer (Kitagawa et al., 2000), and they are known to migrate northward in summer along the coastal regions of Japan and southward for overwintering in the East China Sea and nearshore waters in the Pacific side of Japan (Itoh et al., 2003, Fujioka et al., 2018). The increase of the $\delta^{18}O_{otolith}$ values thus reflects the actual water temperature change experienced by the individuals from autumn to winter. The increasing patterns of the $\delta^{18}O_{otolith}$ in the first year of life observed in this study are consistent with the results previously reported by Shiao et al. (2010), with much greater temporal resolutions (days to weeks) with high precision and accuracy achieved by SIMS techniques.

The $\delta^{18}O_{otolith}$ profiles after the age 0 showed similar seasonal fluctuations, but with much less variation. Figure 3-13 shows monthly averaged water temperature in 2013 at the surface layers (10 to 30 m) in major nursery grounds (Tohoku area and northern Sea of Japan in summer and the East China Sea in winter) of immature bluefin tuna. The estimated water temperature are approximately 8°C higher than the water temperature in respective nursery ground, suggesting that the observed $\delta^{18}O_{otolith}$ profiles after the age 0 is likely due to the effect of thermoregulatory ability developed by Pacific bluefin tuna. For endothermic fish (warm-bodied) such as Pacific bluefin tuna and other tuna species, the $\delta^{18}O_{otolith}$ of immature and adult stages do not merely reflect ambient (*in-situ*) water temperature but, rather, the elevated, internal body temperatures. Using counter current heat

exchangers known as *retia mirabilia* (Dickson & Graham, 2004), bluefin tuna have the capacity to elevate the temperature of their viscera, red (slow-twitch, oxidative) myotomal muscle fibers, eyes, and brain (Linthicum & Carey, 1972, Carey & Lawson, 1973). When juvenile bluefin tuna reach about 20.0 cm in fork length at age-0 (about 2 months after hatching) (Kubo et al., 2008), thermoregulatory ability begins to develop and they are able to maintain their body temperature < 1°C above that of the surrounding water (Furukawa et al., 2017). Thermoregulatory ability of Pacific bluefin tuna increases as fish grow and develop. For example, water temperatures of the peritoneal cavity of adult fish (a 250 kg bluefin tuna) could be 10°C higher than ambient temperatures constructed from acoustic telemetry data (Kitagawa et al., 2006). Since temperatures >35°C are lethal for Pacific bluefin tuna, the observed upper temperature range (30°C) in immature and adult stages is likely a result of physiological thermoregulation to avoid overheating. Understanding how thermoregulatory ability changes with body size and its physiological effects on $\delta^{18}O_{otolith}$ will facilitate better interpretation of the temperature data obtained from this technique.

The estimated temperatures experienced during the larval stages ranged between 26.7°C and 30.7°C among the individuals, with the mean temperature of 28.5 ± 3.0°C (± 2 SD). The field surveys have collected Pacific bluefin tuna larvae in sea surface temperatures (SSTs) between 23.5°C and 29.5°C in the two main spawning grounds (Yonemori 1989, Abe et al., 2014, Suzuki et al., 2014), with higher concentrations of larvae found around 27°C. The estimated temperatures overlap with the range of temperatures observed for larval occurrence of Pacific bluefin tuna. As newly hatched bluefin larvae tend to stay in warm waters within or near the spawning grounds for their optimal growth and survival, temperatures estimated from the core $\delta^{18}O_{otolith}$ corresponding to the early larval period may also serve as a useful indicator of spawning temperatures or the location of spawning grounds. One of the specimens (T64R) appeared to experience relatively warm temperatures (>30°C) associated with decreased growth rates and survival of larvae in the laboratory (Kimura et al., 2007). Although there is evidence that the eggs of Pacific bluefin tuna hatched to normal larvae at 31.5°C in

rearing experiments (Miyashita et al., 2000), the resulted higher temperature estimated for this specimen could be a result of the high-resolution sampling of SIMS which captured several warmer days. Despite the need to increase sample size to accurately judge whether the estimated temperatures are realistic, particularly for the specimens with higher temperature, our results suggest that SIMS $\delta^{18}O_{otolith}$ analysis coupled with a microvolume CF-IRMS $\delta^{18}O_{otolith}$ analysis and a species-specific temperature-dependent fractionation equation is an effective method for reconstructing ambient water temperatures experienced by fish and inferring their early life characteristics, which are difficult to obtain with limited resolutions of the conventional methods.

We developed a novel method to estimate ambient temperatures experienced during the larval stage of fish species using SIMS and microvolume CF-IRMS $\delta^{18}O_{otolith}$ analyses. Microvolume $\delta^{18}O_{otolith}$ analysis revealed that the SIMS $\delta^{18}O_{otolith}$ values were 0.41‰ lower on average than CF-IRMS $\delta^{18}O$ values. High-resolution SIMS $\delta^{18}O_{otolith}$ analysis on Pacific bluefin tuna otoliths achieved greater spatial and temporal resolutions with high precision and accuracy compared to the conventional IRMS methods. The $\delta^{18}O_{otolith}$ profiles of all samples showed distinct seasonal variations, reflecting ambient water temperatures experienced by an individual fish. The developed protocol is useful especially for smaller otoliths with narrow growth increments. SIMS $\delta^{18}O_{otolith}$ analysis coupled with micromilling and microvolume $\delta^{18}O_{otolith}$ analysis allows for microscale examinations of otoliths, and more detailed information on the thermal life history of fish can be obtained compared to conventional IRMS methods. This novel method is a powerful tool for the reconstruction of environmental histories of various fish species and has important implications for understanding how ocean warming is potentially affecting the early life history of fish.

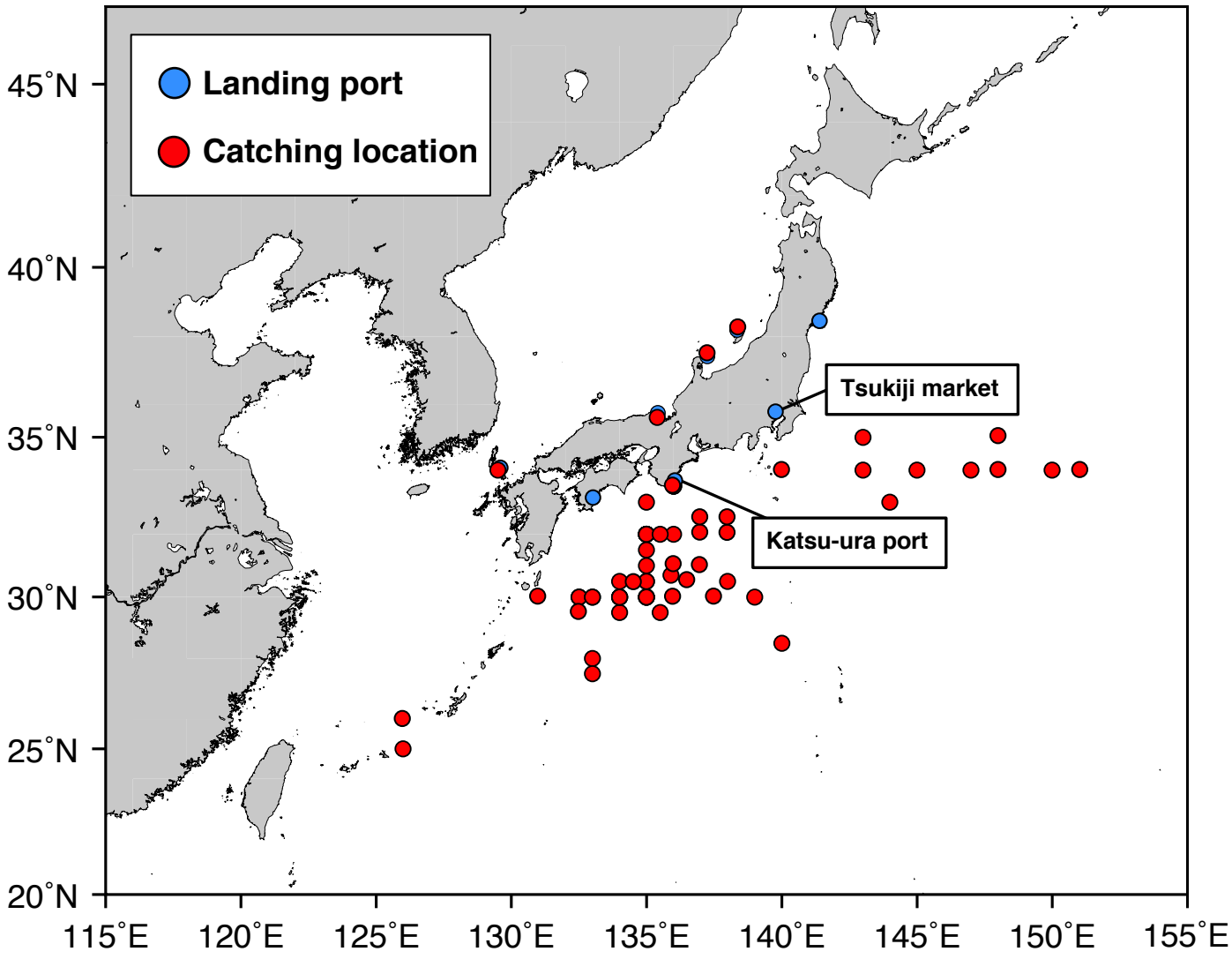

Fig. 3-1. Catch locations and landing ports of Pacific bluefin tuna *Thunnus orientalis* collected in this study.

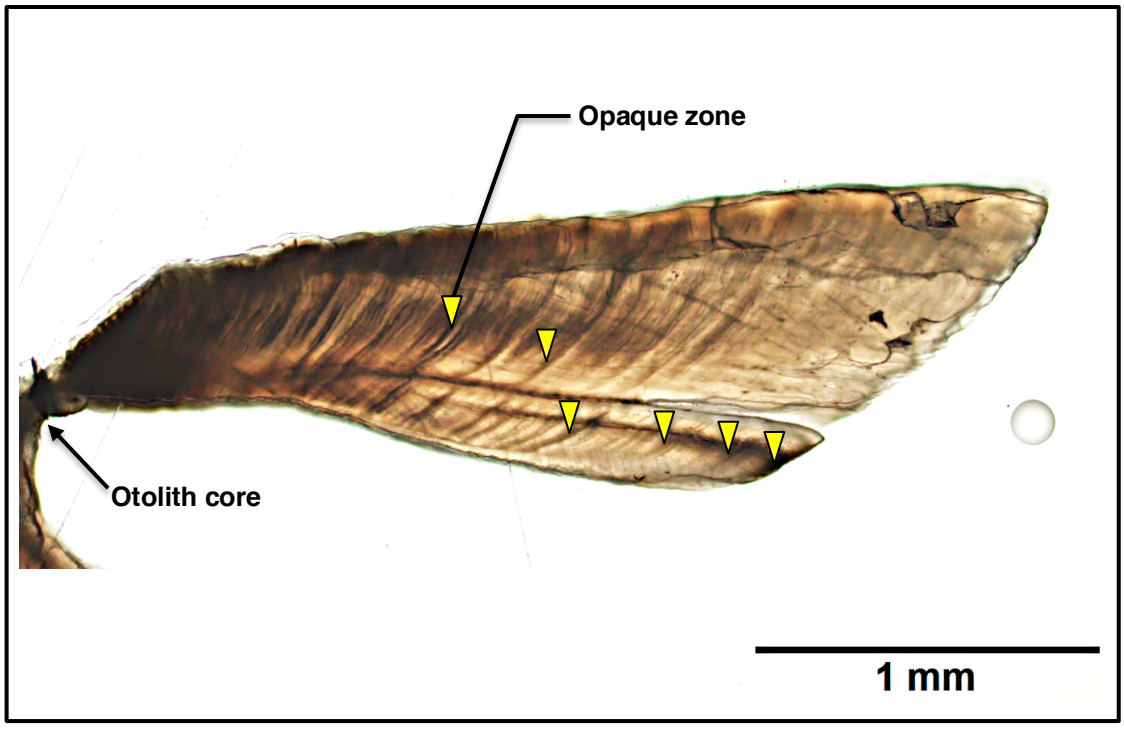

Fig. 3-5. Transverse otolith section of Pacific bluefin tuna *Thunnus orientalis*. Age was determined by counting the number of opaque zones (annual increments) indicated by yellow arrows.

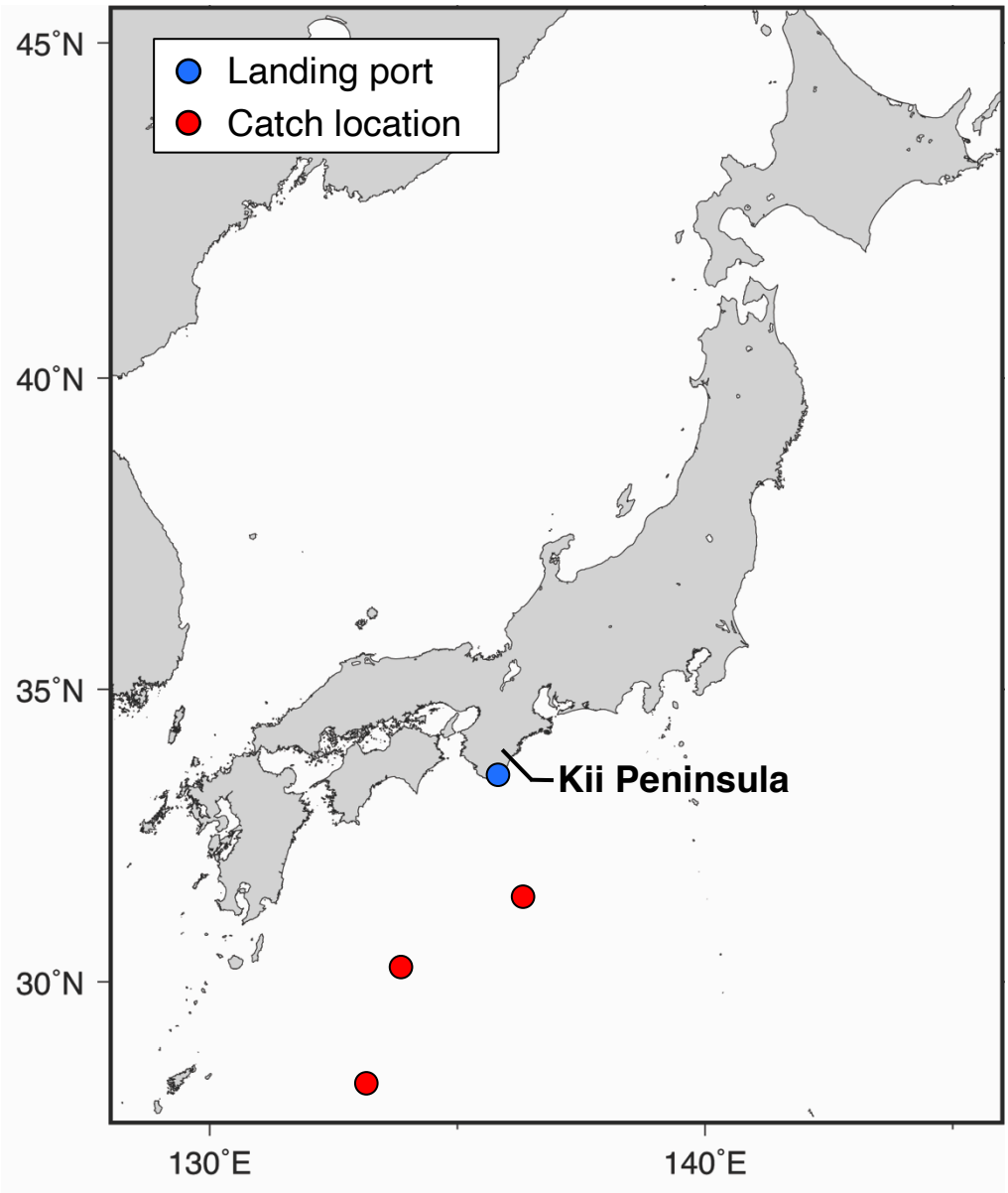

Fig. 3-6. Catch locations of Pacific bluefin tuna *Thunnus orientalis* otolith samples. Two samples (T118R and T131R) were caught in nearshore waters off Kii Peninsula by a small local boat and thus the locations are not shown on the map.

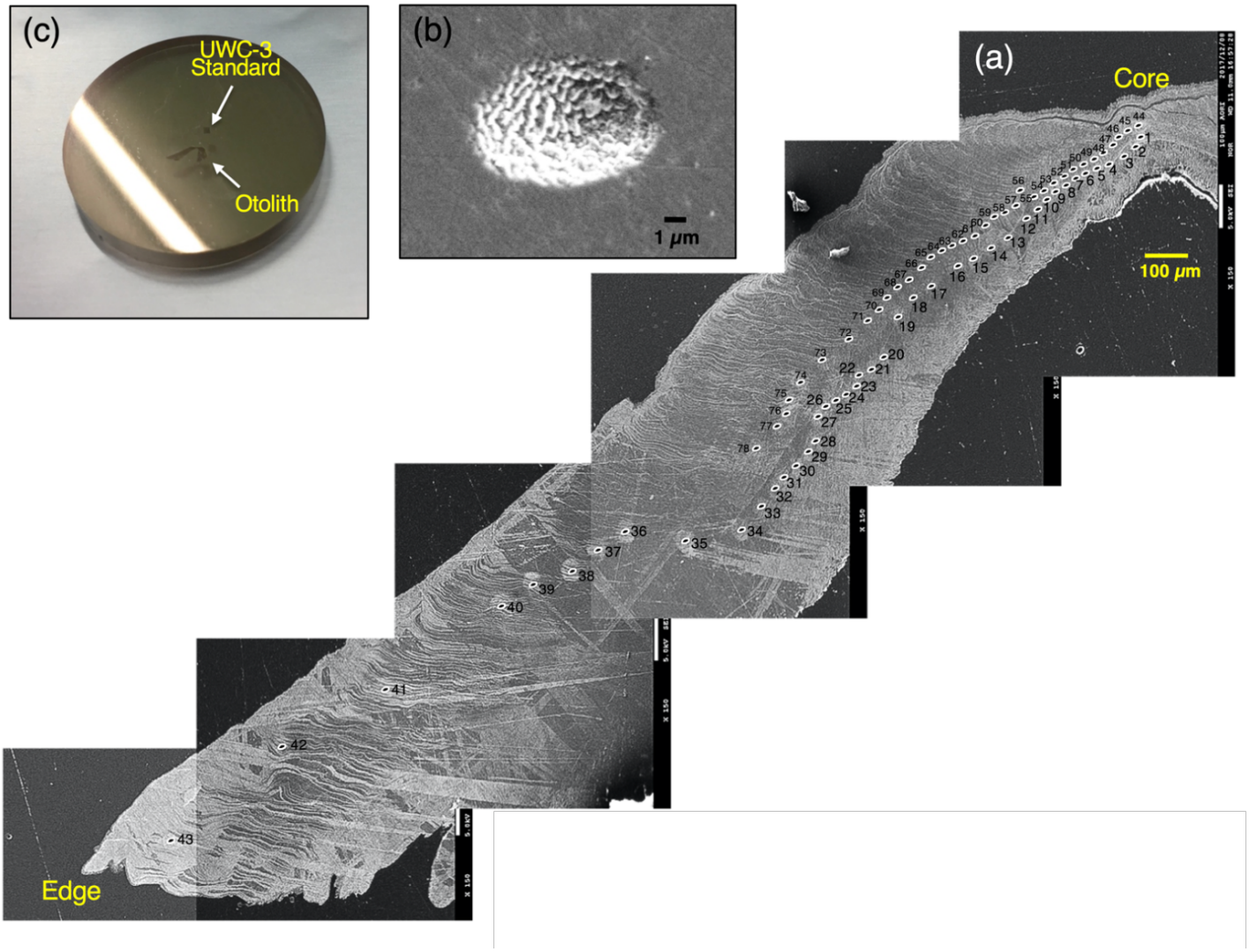

Fig. 3-7. Cross-sectional electron probe micro analyzer (EPMA) image of bluefin tuna otolith with beam spot locations. (b) SIMS beam spot sputtered with a $^{133}Cs^{+}$ primary ion beam focused to a diameter of 10 to 15 μm. (c) Otolith thin section from Pacific bluefin tuna *Thunnus orientalis* embedded in epoxy resin with a calcite UWC-3 standard. The sample surface was mirror-finished and coated with gold.

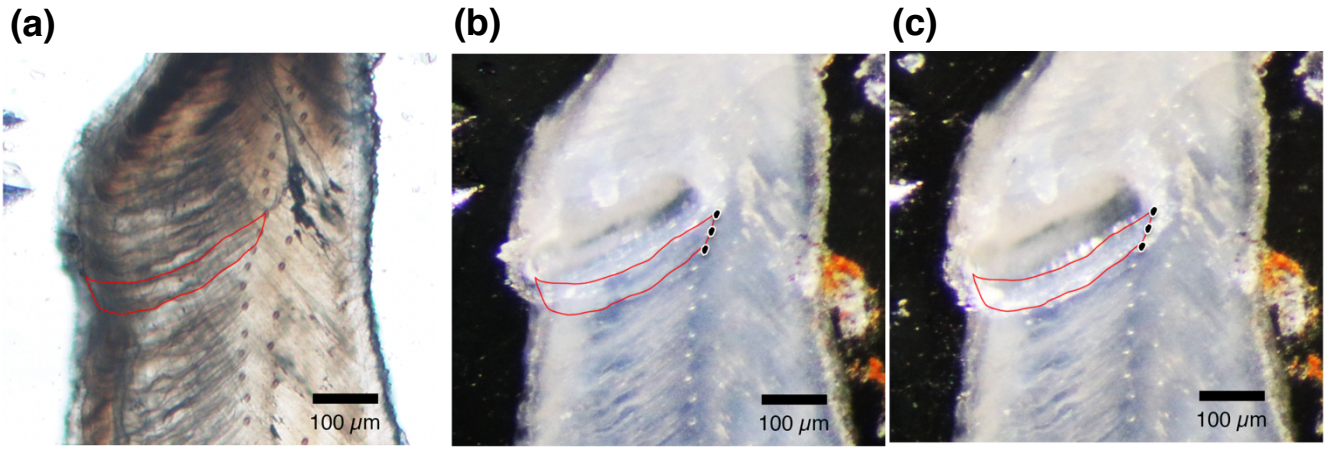

Fig. 3-8. Images of Pacific bluefin tuna *Thunnus orientalis* otolith thin section (T64R) used for micromilling. (a) Before milling, (b) after milling unwanted areas to avoid cross-contamination, (c) and after milling the target milling path (the area inside the red line). Black dots indicate the locations of beam spot where SIMS $\delta^{18}O_{otolith}$ values are stable (−3.01‰, −2.93‰, −3.04‰, respectively from the top to bottom [VPDB]). The images were taken under an optical microscope for (a), and a stereo microscope for (b) and (c).

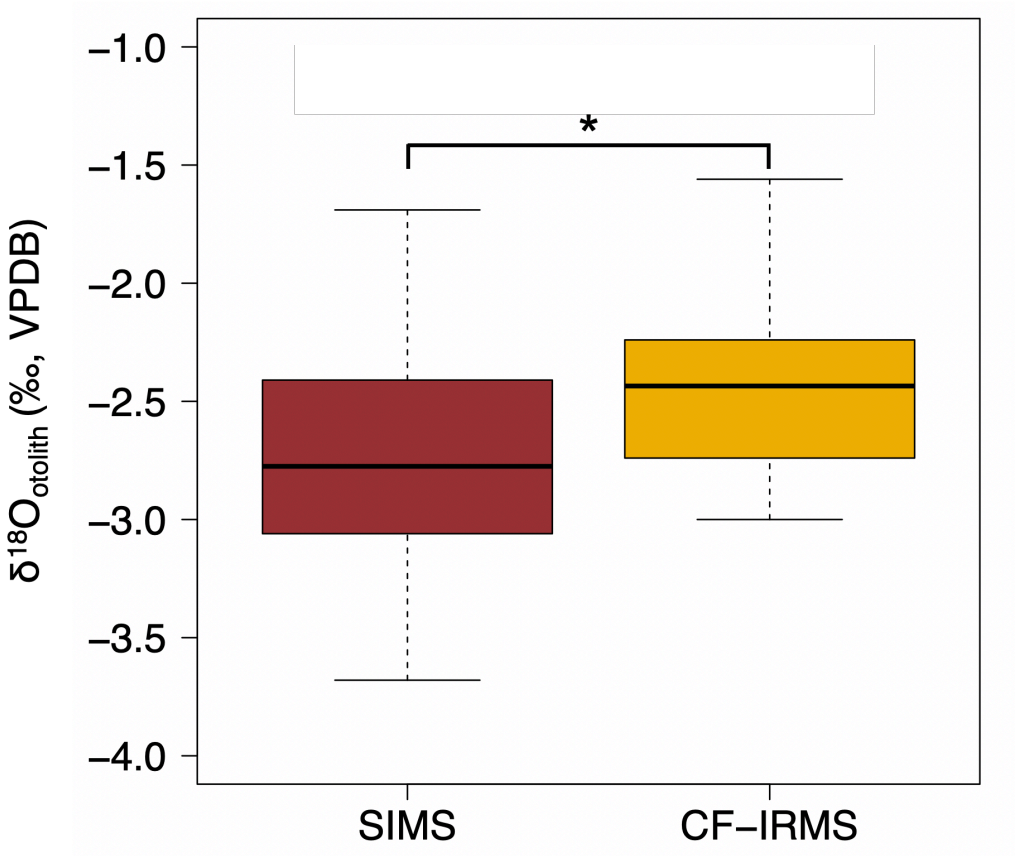

Fig. 3-9. Comparison of SIMS and CF-IRMS $\delta^{18}O_{otolith}$ values (‰, VPDB). (a) CF-IRMS $\delta^{18}O_{otolith}$ values were significantly higher than SIMS $\delta^{18}O_{otolith}$ values (*: Wilcoxon signed-rank test, $p < 0.001$). The bottom and top of the box represent the first (25th percentile) and third (75th percentile) quartiles of the data distribution, respectively. The thick horizontal line inside the box indicates the median, and the upper and lower whiskers represent the maximum and minimum values, respectively.

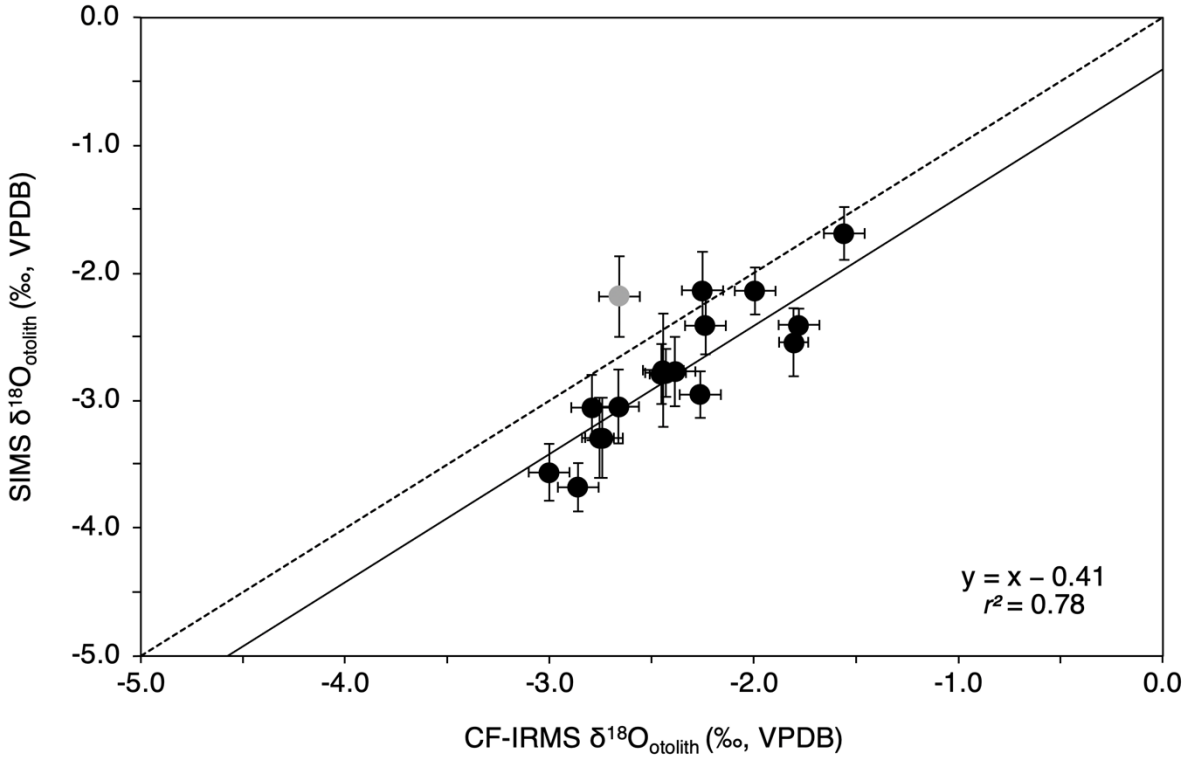

Fig. 3-10. SIMS $\delta^{18}O_{otolith}$ values were 0.41‰ lower on average than CF-IRMS $\delta^{18}O_{otolith}$ values (solid line) when a linear regression with a slope of 1 was fit to the data (r^2 = 0.78). Dashed line indicates 1:1. Horizontal and vertical error bars represent CF-IRMS analytical precision (± 1SD) and propagated error of the average SIMS measurements (± 2SD), respectively. Note that one CF-IRMS $\delta^{18}O_{otolith}$ measurement (grey dot) that had a lower value than the average SIMS $\delta^{18}O_{otolith}$ value was considered as an outlier based on Tukey's outlier detection method and thus excluded for the calculation of the average SIMS–CF-IRMS difference.

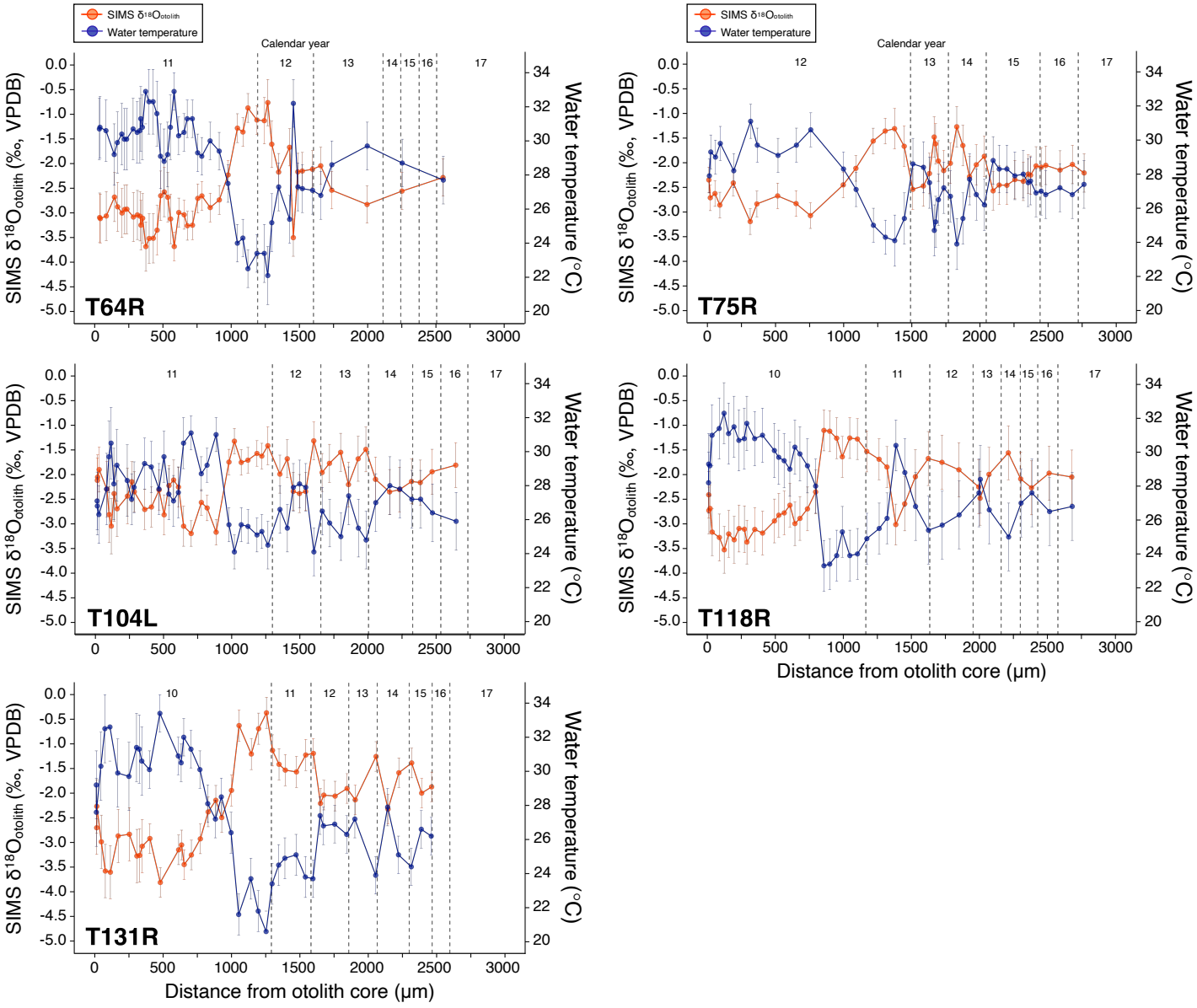

Fig. 3-11. Offset-corrected SIMS $\delta^{18}O_{otolith}$ (‰, VPDB, orange plot on the left y-axis) and reconstructed water temperature (°C, dark blue plot on the right y-axis) of five Pacific bluefin tuna (*Thunnus orientalis*). Error bars represent the spot-to-spot precision of SIMS analyses and the estimated precision of the reconstructed water temperatures (± 2SD). Ambient water temperatures were estimated from the offset-adjusted SIMS $\delta^{18}O_{otolith}$ values using an oxygen fractionation equation for Pacific bluefin larvae proposed by Kitagawa et al. (2013). Dashed vertical lines indicate the locations of annual increments (opaque zone), with numbers showing calendar years of otolith formation. Note $\delta^{18}O_{otolith}$ at the most outer edge was not measured for T104L and T131R, and therefore dashed lines are shown beyond the plots.

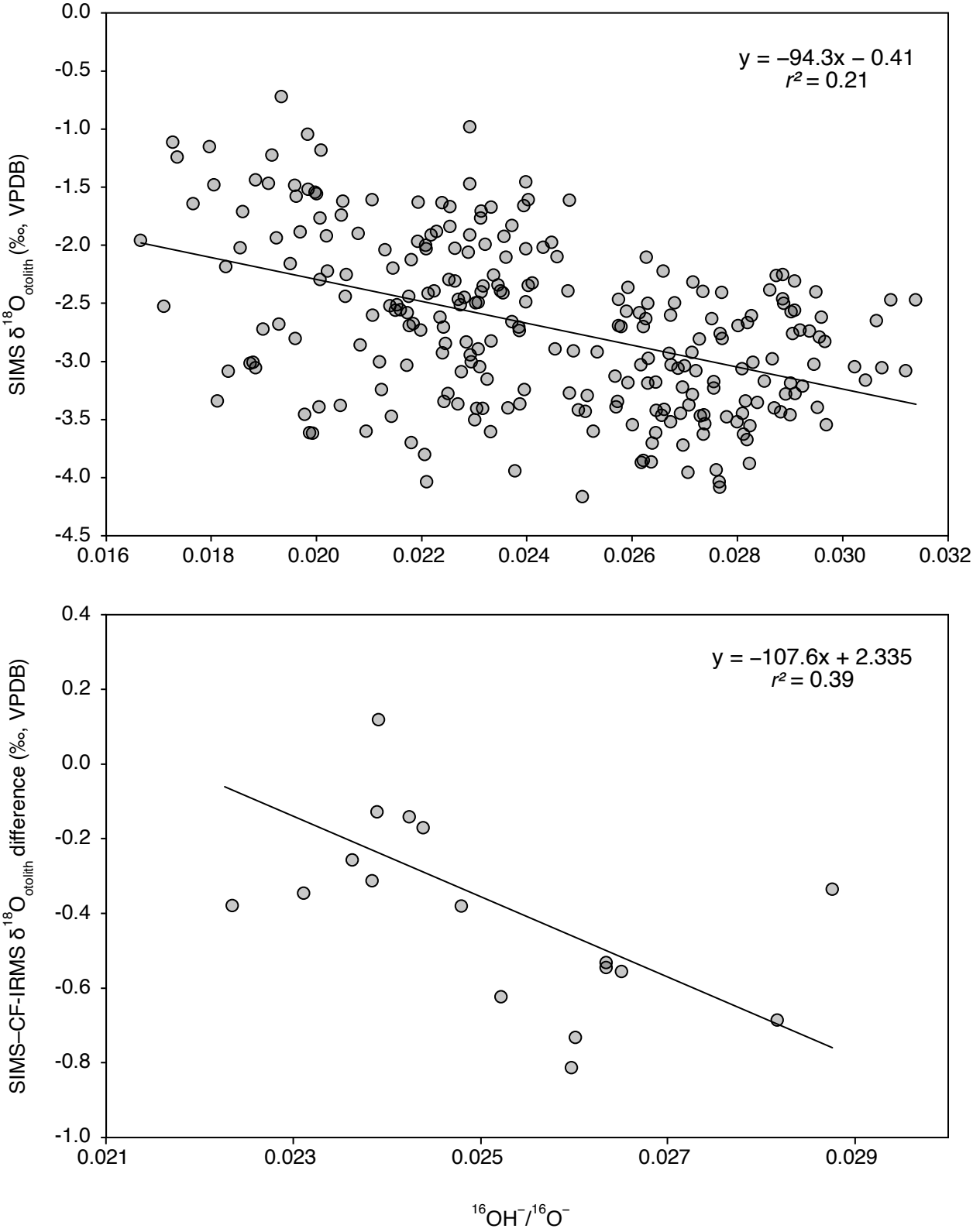

Fig. 3-12. Background-corrected $^{16}OH^{-}/^{16}O^{-}$ plotted against (a) SIMS $\delta^{18}O_{otolith}$ values and (b) SIMS–CF-IRMS $\delta^{18}O_{otolith}$ differences measured for 5 Pacific bluefin tuna (*Thunnus orientalis*) otolith samples.

Table 3. Biological information, sampling data, and number of $\delta^{18}O_{otolith}$ analyses of Pacific bluefin tuna *Thunnus orientalis* used in the present study. Fork length was calculated with a weight-length relationship established by Kai (2007). Two life-history transect lines were analyzed for T64R by SIMS. Numbers in parentheses with asterisks indicate the number of supplementary samples (removed otolith powders that were milled before milling the target milling areas to avoid cross-contamination) analyzed by CF-IRMS.

Sample ID	Catch location	Date of catch	Weight (kg)	Estimated fork length (cm)	Number of SIMS spots	Number of CF-IRMS measurements
T64R	30.0°N, 134.0°E	26 April 2017	146.0	191.1	78 (35 and 43)	5 (2)*
T75R	30.0-32.0°N, 136.0°E	30 April 2017	52.2	136.2	42	–
T104L	27.0-28.0°N, 132.0-134.0°E	18 May 2017	99.2	168.3	53	8 (3)*
T118R	Nearshore off Kii Peninsula	22 May 2017	138.0	187.6	44	9 (4)*
T131R	Nearshore off Kii Peninsula	28 May 2017	118.0	178.2	42	–

CHAPTER 4

Chapter 4 cannot be viewed because the contents will be published in an academic journal.

CHAPTER 5

Chapter 5 cannot be viewed because the contents will be published in an academic journal.

List of references

Abe, O., Masujima, M., Suzuki, N., Morimoto, H., Aonuma, Y., Kameda, T., Segawa, K., Okazaki, M., Iguchi, N., Tanabe, T., Ishihara, T., Watai, M., Ota, T., & Doi, W. (2014). Current status of spawning grounds and periods of Pacific Bluefin Tuna. *Japan Information Papers (ISC/14/Plenary/Info/19)*. Retrieved from http://isc.fra.go.jp/pdf/ISC14/ISC-14-Plenary-INFO-19_JPN_PBF_papers.pdf

Allen, R. (2010). *International management of tuna fisheries: Arrangements, Challenges and a way forward* (FAO Fishereis and Aquaculture Technical Paper No. 536). FAO, Rome. Retrieved from http://www.fao.org/3/i1453e/i1453e00.pdf

Bayliff, W. H, Ishizuki, Y., & Deriso, R. B. (1991). Growth, movement, and attrition of northern bluefin tuna, *Thunnus thynnus*, in the Pacific Ocean, as determined by tagging. *Inter-American Tropical Tuna Commission Bulletin*, *20*(1), 1–94.

Bayliff, W. H. (1994). *A review of the biology and fisheries for northern bluefin tuna, Thunnus thynnus, in the Pacific Ocean* (*FAO Fisheries and Aquaculture Technical Paper No. 336/2*). FAO, Rome. Retrieved from http://www.fao.org/3/T1817E/T1817E13.htm#ch10

Blumberg, A. F., & Mellor, G. L. (1987). A description of a three-dimensional coastal ocean circulation model. *Coastal and Estuarine Sciences*, *4*, 1–16.

Bradley, C. J., Madigan, D. J., Block, B. A., & Popp, B. N. (2014). Amino acid isotope incorporation and enrichment factors in pacific bluefin tuna, *Thunnus orientalis*. *PLOS ONE*, *9*(1). https://doi.org/10.1371/journal.pone.0085818

Campana, S. (1999). Chemistry and composition of fish otoliths: pathways, mechanisms and applications. *Marine Ecology Progress Series*, *188*, 263–297. https://doi.org/10.3354/meps188263

Campana, S. E., & Neilson, J. D. (1985). Microstructure of fish otoliths. *Canadian Journal of Fisheries and Aquatic Sciences*, *42*(5), 1014–1032. https://doi.org/10.1139/f85-127

Carey, F. G., & Lawson, K. D. (1973). Temperature regulation in free-swimming bluefin tuna. *Comparative Biochemistry and Physiology Part A: Physiology*, *44*(2), 375–392. https://doi.org/10.1016/0300-9629(73)90490-8

Chen, K. S., Crone, P., & Hsu, C. C. (2006). Reproductive biology of female Pacific bluefin tuna *Thunnus orientalis* from south-western North Pacific Ocean. *Fisheries Science*, *72*(5), 985–994. https://doi.org/10.1111/j.1444-2906.2006.01247.x

Chung, M. T., Trueman, C. N., Godiksen, J. A., & Grønkjær, P. (2019a). Otolith $\delta^{13}C$ values as a metabolic proxy: Approaches and mechanical underpinnings. *Marine and Freshwater Research*, *70*(12), 1747–1756. https://doi.org/10.1071/MF18317

Chung, M. T., Trueman, C. N., Godiksen, J. A., Holmstrup, M. E., & Grønkjær, P. (2019b). Field metabolic rates of teleost fishes are recorded in otolith carbonate. *Communications Biology*, *2*(1), 1–10. https://doi.org/10.1038/s42003-018-0266-5

Coplen, T. B., Kendall, C., & Hopple, J. (1983). Comparison of stable isotope reference samples. *Nature*, *302*, 236–238.

Devereux, I. (1967). Temperature Measurements from Oxygen Isotope Ratios of Fish Otoliths. *Science*, *155*(3770), 1684–1685. https://doi.org/10.1126/science.155.3770.1684

Dickson, K. A., & Graham, J. B. (2004). Evolution and Consequences of Endothermy in Fishes. *Physiological and Biochemical Zoology*, *77*(6), 998–1018. https://doi.org/10.1086/423743

Dufour, E., Höök, T. O., Patterson, W. P., & Rutherford, E. S. (2008). High-resolution isotope analysis of young alewife *Alosa pseudoharengus* otoliths: Assessment of temporal resolution and reconstruction of habitat occupancy and thermal history. *Journal of Fish Biology*, *73*(10), 2434–2451. https://doi.org/10.1111/j.1095-8649.2008.02090.x

Eiler, J. M., Graham, C., & Valley, J. W. (1997). SIMS analysis of oxygen isotopes: Matrix effects in complex minerals and glasses. *Chemical Geology*, *138*(3–4), 221–244. https://doi.org/10.1016/S0009-2541(97)00015-6

Fujioka, K., Fukuda, H., Furukawa, S., Tei, Y., Okamoto, S., & Ohshimo, S. (2018). Habitat use and

movement patterns of small (age-0) juvenile Pacific bluefin tuna (*Thunnus orientalis*) relative to the Kuroshio. *Fisheries Oceanography*, *27*(3), 185–198. https://doi.org/10.1111/fog.12244

Fujioka, K., Masujima, M., Boustany, A.M., & Kitagawa, T. (2015). Horizontal movements of Pacific bluefin tuna. In T. Kitagawa. & S. Kimura. (Eds.), *Biology and ecology of bluefin tuna* (pp. 101–122). CRC Press, Boca Raton London, New York.

Furukawa, S., Fujioka, K., Fukuda, H., Suzuki, N., Tei, Y., & Ohshimo, S. (2017). Archival tagging reveals swimming depth and ambient and peritoneal cavity temperature in age-0 Pacific bluefin tuna, *Thunnus orientalis*, off the southern coast of Japan. *Environmental Biology of Fishes*, *100*, 35–48. https://doi.org/10.1007/s10641-016-0552-3

Geffen, A. J. (2012). Otolith oxygen and carbon stable isotopes in wild and laboratory-reared plaice (*Pleuronectes platessa*). *Environmental Biology of Fishes*, *95*(4), 419–430. https://doi.org/10.1007/s10641-012-0033-2

Godiksen, J. A., Svenning, M.-A., Dempson, J. B., Marttila, M., Storm-Suke, A., & Power, M. (2010). Development of a species-specific fractionation equation for Arctic charr (*Salvelinus alpinus* (L.)): an experimental approach. *Hydrobiologia*, *650*(1), 67–77. https://doi.org/10.1007/s10750-009-0056-7

Hane, Y. (2016). Analyses of local-scale migration of tuna species based on historical archives and its mechanism related to oceanic environmental fluctuations in Japan. MSc dissertation, The University of Tokyo, Kashiwa, Chiba (in Japanese)

Hane, Y., Kimura, S., Yokoyama, Y., Miyairi, Y., Ushikubo, T., Ishimura, T., Ogawa, N., Aono, T., & Nishida, K. (2020). Reconstruction of temperature experienced by Pacific bluefin tuna *Thunnus orientalis* larvae using SIMS and microvolume CF-IRMS otolith oxygen isotope analyses. *Marine Ecology Progress Series*, *649*, 175–188. https://doi.org/10.3354/meps13451

Hanson, N., Wurster, C., EIMF, & Todd, C. (2010). Comparison of secondary ion mass spectrometry and micromilling/continuous flow isotope ratio mass spectrometry techniques used to acquire intra-otolith $\delta^{18}O$ values of wild Atlantic salmon (*Salmo salar*). *Rapid Communications in Mass Spectrometry*, *24*, 1457–1466. https://doi.org/10.1002/rcm

Hanson, N. N., Wurster, C. M., Eimf, & Todd, C. D. (2013). Reconstructing marine life-history strategies of wild Atlantic salmon from the stable isotope composition of otoliths. *Marine Ecology Progress Series*, *475*, 249–266. https://doi.org/10.3354/meps10066

Helser, T. E., Kastelle, C. R., McKay, J. L., Orland, I. J., Kozdon, R., & Valley, J. W. (2018). Evaluation of micromilling/conventional isotope ratio mass spectrometry and secondary ion mass spectrometry of $\delta^{18}O$ values in fish otoliths for sclerochronology. *Rapid Communications in Mass Spectrometry*, *32*(20), 1781–1790. https://doi.org/10.1002/rcm.8231

Helser, T., Kastelle, C., Crowell, A., Ushikubo, T., Orland, I. J., Kozdon, R., & Valley, J. W. (2018). A 200-year archaeozoological record of Pacific cod (*Gadus macrocephalus*) life history as revealed through ion microprobe oxygen isotope ratios in otoliths. *Journal of Archaeological Science: Reports*, *21*(November 2016), 1236–1246. https://doi.org/10.1016/j.jasrep.2017.06.037

Høie, H., Otterlei, E., & Folkvord, A. (2004). Temperature-dependent fractionation of stable oxygen isotopes in otoliths of juvenile cod (*Gadus morhua L.*). *ICES Journal of Marine Science*, *61*(2), 243–251. https://doi.org/10.1016/j.icesjms.2003.11.006

Horikawa, K., Kodaira, T., Zhang, J., & Murayama, M. (2015). $\delta^{18}O_{sw}$ estimate for *Globigerinoides ruber* from core-top sediments in the East China Sea. *Progress in Earth and Planetary Science*, *2*(1). https://doi.org/10.1186/s40645-015-0048-3

Hüssy, K., Limburg, K. E., de Pontual, H., Thomas, O. R. B., Cook, P. K., Heimbrand, Y., Blass, M., & Sturrock, A. M. (2020). Trace Element Patterns in Otoliths: The Role of Biomineralization. *Reviews in Fisheries Science & Aquaculture*, 1–33. https://doi.org/10.1080/23308249.2020.1760204

Hut, G. (1987). Consultants' group meeting on stable isotope reference samples for geochemical and hydrological investigations. IAEA, Vienna, Retrieved from http://www.iaea.org/inis/collection/NCLCollectionStore/_Public/18/075/18075746.pdf

Imsland, A. K., Ólafsson, K., Skírnisdóttir, S., Gunnarsson, S., Oddgeirsson, M., Vandamme, S., Helyar, S. J., Skadal, J., & Folkvord, A. (2014). Life history of turbot in Icelandic waters: Intra- and inter-population genetic diversity and otolith tracking of environmental temperatures. *Fisheries Research*, *155*, 185–193. https://doi.org/10.1016/j.fishres.2014.03.004

International Scientific Committee for Tuna and Tuna-Like Species in the North Pacific Ocean. (2020). *Stock aseessment of Pacific bluefin tuna in the Pacific Ocean in 2020*.

Ishimura, T., Tsunogai, U., & Gamo, T. (2004). Stable carbon and oxygen isotopic determination of sub-microgram quantities of $CaCO_3$ to analyze individual foraminiferal shells. *Rapid Communications in Mass Spectrometry*, *18*(23), 2883–2888. https://doi.org/10.1002/rcm.1701

Ishimura, T., Tsunogai, U., & Nakagawa, F. (2008). Grain-scale heterogeneities in the stable carbon and oxygen isotopic compositions of the international standard calcite materials (NBS 19, NBS 18, IAEA-CO-1, and IAEA-CO-8). *Rapid Communications in Mass Spectrometry*, *22*, 1925–1932. https://doi.org/10.1002/rcm

Itoh, T., Tsuji, S., & Nitta, A. (2003). Migration patterns of young Pacific bluefin tuna (*Thunnus orientalis*) determined with archival tags. *Fisheries Bulletin (Washington D.C.)*, *101*(3), 514–534.

IUCN 2020. The IUCN Red List of Threatened Species. Version 2020-2. https://www.iucnredlist.org. Downloaded on 05 March 2020.

Jones, B. J., & Campana, S. E. (2009). Stable oxygen isotope reconstruction of ambient temperature during the collapse of a cod (*Gadus morhua*) fisher. *Ecological Applications*, *19*(6), 1500–1514.

Kai, M. (2007). Weight-length relationship of North Western Pacific bluefin tuna. *Working Group Working Papers (ISC/07/PBF-3/07)*. Retrieved from http://isc.fra.go.jp/pdf/PBF/ISC07_PBF_3/ISC_07_PBFWG3_07.pdf

Kalish, J. M. (1991a). Marine Biology Oxygen and carbon stable isotopes in the otoliths. *Marine Biology*, *110*, 37–47.

Kalish, J. M. (1991b). Oxygen and carbon stable isotopes in the otoliths of wild and laboratory-reared Australian salmon (*Arripis trutta*). *Marine Biology*, *110*, 37–47.

Kawazu, M., Tawa, A., Ishihara, T. et al. (2020). Discrimination of eastward trans-Pacific migration of the Pacific bluefin tuna *Thunnus orientalis* through otolith $\delta^{13}C$ and $\delta^{18}O$ analyses. *Marine*

Biology 167, 110. https://doi.org/10.1007/s00227-020-03723-9

Kim, S. T., Coplen, T. B., & Horita, J. (2015). Normalization of stable isotope data for carbonate minerals: Implementation of IUPAC guidelines. *Geochimica et Cosmochimica Acta*, *158*, 276–289. https://doi.org/10.1016/j.gca.2015.02.011

Kimura, S., Kato, Y., Kitagawa, T., & Yamaoka, N. (2010). Impacts of environmental variability and global warming scenario on Pacific bluefin tuna (*Thunnus orientalis*) spawning grounds and recruitment habitat. *Progress in Oceanography*, *86*(1–2), 39–44. https://doi.org/10.1016/j.pocean.2010.04.018

Kimura, S., Kiagawa, T., Kato, Y., & Yamaoka, N. (2007). Fluctuation in spawning environment of bluefin tuna and Japanese eel associated with global warming and their ecological response. *Kaiyo Monthly*, *39*, 317–322 (in Japanese).

Kita, N. T., Ushikubo, T., Fu, B., & Valley, J. W. (2009). High precision SIMS oxygen isotope analysis and the effect of sample topography. *Chemical Geology*, *264*(1–4), 43–57. https://doi.org/10.1016/j.chemgeo.2009.02.012

Kitagawa, T., Nakata, H., Kimura, S., Itoh, T., Tsuji, S., & Nitta, A. (2000). Effect of ambient temperature on the vertical distribution and movement of Pacific bluefin tuna *Thunnus thynnus* orientalis. *Marine Ecology Progress Series*, *206*, 251–260. https://doi.org/10.3354/meps206251

Kitagawa, T., Ishimura, T., Uozato, R., Shirai, K., Amano, Y., Shinoda, A., Otake, Tsuguo., Tsunogai, U., & Kimura, S. (2013). Otolith $\delta^{18}O$ of Pacific bluefin tuna *Thunnus orientalis* as an indicator of ambient water temperature. *Marine Ecology Progress Series*, *481*(Anon 2010), 199–209. https://doi.org/10.3354/meps10202

Kitagawa, Takashi, Kato, Y., Miller, M. J., Sasai, Y., Sasaki, H., & Kimura, S. (2010). The restricted spawning area and season of Pacific bluefin tuna facilitate use of nursery areas: A modeling approach to larval and juvenile dispersal processes. *Journal of Experimental Marine Biology and Ecology*, *393*(1–2), 23–31. https://doi.org/10.1016/j.jembe.2010.06.016

Kitagawa, Takashi, Kimura, S., Nakata, H., & Yamada, H. (2006a). Thermal adaptation of Pacific bluefin tuna *Thunnus orientalis* to temperate waters. *Fisheries Science*, *72*(1), 149–156.

https://doi.org/10.1111/j.1444-2906.2006.01129.x

Kitagawa, Takashi, Kimura, S., Nakata, H., & Yamada, H. (2006b). Thermal adaptation of Pacific bluefin tuna *Thunnus orientalis* to temperate waters. *Fisheries Science*, *72*(1), 149–156. https://doi.org/10.1111/j.1444-2906.2006.01129.x

Kodaira, T., Horikawa, K., Zhang, J., & Senjyu, T. (2016). Relationship between seawater oxygen isotope ratio and salinity in the Tsushima Current, the Sea of Japan. *Chikyukagaku (Geochemistry)*, *50*, 263–277. https://doi.org/10.14934/chikyukagaku.50.263 (in Japanese).

Kozdon, R., Ushikubo, T., Kita, N. T., Spicuzza, M., & Valley, J. W. (2009a). Intratest oxygen isotope variability in the planktonic *foraminifer N. pachyderma*: Real vs. apparent vital effects by ion microprobe. *Chemical Geology*, *258*(3–4), 327–337. https://doi.org/10.1016/j.chemgeo.2008.10.032

Kubo, T., Sakamoto, W., Murata, O., & Kumai, H. (2008). Whole-body heat transfer coefficient and body temperature change of juvenile Pacific bluefin tuna *Thunnus orientalis* according to growth. *Fisheries Science*, *74*(5), 995–1004. https://doi.org/10.1111/j.1444-2906.2008.01617.x

Ladich, F., and Popper, A. N. (2004). Parallel evolution in fish hearing organs. In G. A. Manley, A. N. Popper & R. R. Fay (Eds.), *Evolution of the Vertebrate Auditory System* (pp. 95–127). Springer, New York.

Limburg, K. E., Hayden, T. A., Pine, W. E., Yard, M. D., Kozdon, R., & Valley, J. W. (2013). Of travertine and time: Otolith chemistry and microstructure detect provenance and demography of endangered humpback chub in Grand Canyon, USA. *PLOS ONE*, *8*(12), 1–18. https://doi.org/10.1371/journal.pone.0084235

Linthicum, D. S., & Carey, F. G. (1972). Regulation of brain and eye temperatures by the bluefin tuna. *Comparative Biochemistry and Physiology Part A: Physiology*, *43*(2), 425–433. https://doi.org/10.1016/0300-9629(72)90201-0

Linzmeier, B. J., Kozdon, R., Peters, S. E., & Valley, J. W. (2016). Oxygen isotope variability within nautilus shell growth bands. *PLOS ONE*, *11*(4), 1–31. https://doi.org/10.1371/journal.pone.0153890

Madigan, D. J., Baumann, Z., Carlisle, A. B., Snodgrass, O., Dewar, H., & Fisher, N. S. (2018). Isotopic insights into migration patterns of Pacific bluefin tuna in the eastern Pacific Ocean. *Canadian Journal of Fisheries and Aquatic Sciences*, *75*(2), 260–270. https://doi.org/10.1139/cjfas-2016-0504

Madigan, D. J., Boustany, A., & Collette, B. B. (2017). East not least for Pacific bluefin tuna. *Science*, *357*(6349), 356–357. https://doi.org/10.1126/science.aan3710

Matta, M. E., Orland, I. J., Ushikubo, T., Helser, T. E., Black, B. A., & Valley, J. W. (2013). Otolith oxygen isotopes measured by high-precision secondary ion mass spectrometry reflect life history of a yellowfin sole (*Limanda aspera*). *Rapid Communications in Mass Spectrometry*, *27*(6), 691–699. https://doi.org/10.1002/rcm.6502

Miyashita, S., Tanaka, Y., Sawada, Y., Takii, K., Mukai, Y., & Kumai, H. (2000). Embryonic Development and Effects of Water Temperature on Hatching of the Bluefin Tuna, *Thunnus thynnus*. *Aquaculture Science*, *48*(2), 199–207. https://doi.org/10.11233/aquaculturesci1953.48.199

Morales-Nin, B. Y. O. (1986). Structure and composition of otoliths of Cape hake Merluccius capensis. *South African Journal of Marine Science*, *4*(1), 3–10. https://doi.org/10.2989/025776186784461639

Moyano, M., Candebat, C., Ruhbaum, Y., Álvarez-Fernández, S., Claireaux, G., Zambonino-Infante, J. L., & Peck, M. A. (2017). Effects of warming rate, acclimation temperature and ontogeny on the critical thermal maximum of temperate marine fish larvae. *PLOS ONE*, *12*(7), 1–23. https://doi.org/10.1371/journal.pone.0179928

Muhling, B. A., Lee, S. K., Lamkin, J. T., & Liu, Y. (2011). Predicting the effects of climate change on bluefin tuna (*Thunnus thynnus*) spawning habitat in the Gulf of Mexico. *ICES Journal of Marine Science*, *68*(6), 1051–1062. https://doi.org/10.1093/icesjms/fsr008

Muhling, B. A., Liu, Y., Lee, S. K., Lamkin, J. T., Roffer, M. A., Muller-Karger, F., & Walter, J. F. (2015). Potential impact of climate change on the Intra-Americas Sea: Part 2. Implications for Atlantic bluefin tuna and skipjack tuna adult and larval habitats. *Journal of Marine Systems*,

148, 1–13. https://doi.org/10.1016/j.jmarsys.2015.01.010

Murayama, E., Okuno, A., Ohira, T., Takagi, Y., & Nagasawa, H. (2000). Molecular cloning and expression of an otolith matrix protein cDNA from the rainbow trout, *Oncorhynchus mykiss*. *Comparative Biochemistry and Physiology Part B: Biochemistry and Molecular Biology*, *126*(4), 511–520. https://doi.org/10.1016/S0305-0491(00)00223-6

Murayama, E., Takagi, Y., Ohira, T., Davis, J. G., Greene, M. I., & Nagasawa, H. (2002). Fish otolith contains a unique structural protein, otolin-1. *European Journal of Biochemistry*, *269*(2), 688–696. https://doi.org/10.1046/j.0014-2956.2001.02701.x

Nishida, K., & Ishimura, T. (2017). Grain-scale stable carbon and oxygen isotopic variations of the international reference calcite, IAEA-603. *Rapid Communications in Mass Spectrometry*, *31*(22), 1875–1880. https://doi.org/10.1002/rcm.7966

Ohshimo, S., Tawa, A., Ota, T., Nishimoto, S., Ishihara, T., Watai, M., Satoh, K., Tanabe, T., & Abe, O. (2017a). Horizontal distribution & habitat of Pacific bluefin tuna, *Thunnus orientalis*, larvae in the waters around Japan. *Bulletin of Marine Science*, *93*(3), 769–787. https://doi.org/10.5343/bms.2016.1094

Ohshimo, S., Sato, T., Okochi, Y., Tanaka, S., Ishihara, T., Ashida, H., & Suzuki, N. (2018). Evidence of spawning among Pacific bluefin tuna, *Thunnus orientalis*, in the Kuroshio and Kuroshio-Oyashio transition area. *Aquatic Living Resources*, *31*(33). https://doi.org/10.1051/alr/2018022

Okiyama, M. (1974). Occurrence of the postlarvae of bluefin tuna *Thunnus thynnus* in the Japan Sea. *Bulletin of the Japan Sea Regional Fisheries Research Laboratory*. *25*, 89–97

Okochi, Y., Abe, O., Tanaka, S., Ishihara, Y., & Shimizu, A. (2016). Reproductive biology of female Pacific bluefin tuna, *Thunnus orientalis*, in the Sea of Japan. *Fisheries Research*, *174*, 30–39. https://doi.org/10.1016/j.fishres.2015.08.020

Orland, I. J., Kozdon, R., Linzmeier, B., Wycech, J., Śliwiński, M., Kitajima, K., Kita, N., & Valley, J. W. (2015) Enhancing the accuracy of carbonate $\delta^{18}O$ and $\delta^{13}C$ measurements by SIMS. Am Geophys Union. Washington DC, Presentation PP52B-03.

https://ui.adsabs.harvard.edu/abs/2015AGUFMPP52B..03O/abstract (accessed 20 Mar 2019)

Pankhurst, N. W., & Munday, P. L. (2011). Effects of climate change on fish reproduction and early life history stages. *Australian Journal of Marine and Freshwater Research*, *62*(9), 1015–1026. https://doi.org/10.1071/MF10269

Patterson, W. P., Smith, G. R., & Lohmann, K. C. (1993). Continental Paleothermometry and Seasonality Using the Isotopic Composition of Aragonitic Otoliths of Freshwater Fishes. *Geophysical Monograph*, 191–202. https://doi.org/10.1029/gm078p0191

Perry, A. L., Low, P. J., Ellis, J. R., & Reynolds, J. D. (2005). Climate change and distribution shifts in marine fishes. *Science*, *308*(5730), 1912–1915. https://doi.org/10.1126/science.1111322

Pörtner, H. O., & Peck, M. A. (2010). Climate change effects on fishes and fisheries: Towards a cause-and-effect understanding. *Journal of Fish Biology*, *77*(8), 1745–1779. https://doi.org/10.1111/j.1095-8649.2010.02783.x

Popper, A. N., Fay, R. R., Platt, C., & Sand, O. (2003). Sound detection mechanisms and capabilities of teleost fishes. In S. P. Collin & N. J. Marshall (Eds.), *Sensory Processing in Aquatic Environments* (pp. 3–38). Springer-Verlag, New York.)

Radtke, R. L., Showers, W., Moksness, E., & Lenz, P. (1996). Environmental information stored in otoliths: Insights from stable isotopes. *Marine Biology*, *127*(1), 161–170. https://doi.org/10.1007/BF00993656

Radtke, R. L., Showers, W., Moksness, E., & Lenz, P. (1998). Corrigendum: Environmental information stored in otoliths: insights from stable isotopes. *Marine Biology*, *132*, 347–348. Retrieved from http://link.springer.com/10.1007/BF00993656

Riciputi, L. R., Paterson, B. A., & Ripperdan, R. L. (1998). Measurement of light stable isotope ratios by SIMS: Matrix effects for oxygen, carbon, and sulfur isotopes in minerals. *International Journal of Mass Spectrometry*, *178*(1–2), 81–112. https://doi.org/10.1016/S1387-3806(98)14088-5

Rooker, J., Secor, D., De Metrio, G., Rodríquez-Marín, E., & Farrugia, A. F. (2006). Evaluation of

population structure and mixing rates of Atlantic bluefin tuna from chemical signatures in otoliths. *Collective Volume of Scientific Papers ICCAT*, *59(3)*(3), 813–818. Retrieved from https://www.iccat.int/Documents/CVSP/CV059_2006/n_3/CV059030813.pdf

Rooker, J. R, & Secor, D. H. (2004). Stock Structure and Mixing of Altantic Bluefin Tuna : Evidence From Stable $\delta^{13}C$ and $\delta^{18}O$ Isotopes in Otoliths. *Collected Volume of Scientific Papers ICCAT*, *56*(3), 1115–1120.

Rooker, J. R., Secor, D. H., Zdanowicz, V. S., De Metrio, G., Orsi Relini, L., Deflorio, M., Santamaria, N., Palandri, G., & Relini, M. (2002). Otolith elemental fingerprint of atlantic bluefin tuna from Eastern and Western nurseries. *Collective Volume of Scientifi Papers ICCAT*, *54*(2), 9 pp.

Rooker, J. R., Secor, D. H., DeMetrio, G., Kaufman, A. J., Ríos, A. B., & Tičina, V. (2008). Evidence of trans-Atlantic movement and natal homing of bluefin tuna from stable isotopes in otoliths. *Marine Ecology Progress Series*, *368*, 231–239. https://doi.org/10.3354/meps07602

Rooker, J. R., Secor, D. H., Zdanowicz, V. S., De Metrio, G., & Relini, L. O. (2003). Identification of Atlantic bluefin tuna (*Thunnus thynnus*) stocks from putative nurseries using otolith chemistry. *Fisheries Oceanography*, *12*(2), 75–84. https://doi.org/10.1046/j.1365-2419.2003.00223.x

Sakamoto, T., Komatsu, K., Yoneda, M., Ishimura, T., Higuchi, T., Shirai, K., Kamimura, Y., Watanabe, C., & Kawabata, A. (2017). Temperature dependence of $\delta^{18}O$ in otolith of juvenile Japanese sardine: Laboratory rearing experiment with micro-scale analysis. *Fisheries Research*, *194*(May), 55–59. https://doi.org/10.1016/j.fishres.2017.05.004

Sakamoto, T., Komatsu, K., Shirai, K., Higuchi, T., Ishimura, T., Setou, T., Kamimura, Y., & Kawabata, A. (2019). Combining microvolume isotope analysis and numerical simulation to reproduce fish migration history. *Methods in Ecology and Evolution*, *10*(1), 59–69. https://doi.org/10.1111/2041-210X.13098

Sano, Y., Shirai, K., Takahata, N., Amakawa, H., & Otake, T. (2008). Ion microprobe Sr isotope analysis of carbonates with about 5 μm spatial resolution: An example from an ayu otolith. *Applied Geochemistry*, *23*(8), 2406–2413. https://doi.org/10.1016/j.apgeochem.2008.02.027

Satoh, K. (2010). Horizontal and vertical distribution of larvae of Pacific bluefin tuna *Thunnus orientalis* in patches entrained in mesoscale eddies. *Marine Ecology Progress Series*, *404*, 227–240. https://doi.org/10.3354/meps08431

Secor, D. H., Campana, S. E., Zdanowicz, V. S., Lam, J. W. H., Yang, L., & Rooker, J. R. (2002). Inter-laboratory comparison of Atlantic and Mediterranean bluefin tuna otolith microconstituents. *ICES Journal of Marine Science*, *59*(6), 1294–1304. https://doi.org/10.1006/jmsc.2002.1311

Shephard, S., Trueman, C., Rickaby, R., & Rogan, E. (2007). Juvenile life history of NE Atlantic orange roughy from otolith stable isotopes. *Deep-Sea Research Part I*, *54*(8), 1221–1230. https://doi.org/10.1016/j.dsr.2007.05.007

Shiao, J. C., Itoh, S., Yurimoto, H., Iizuka, Y., & Liao, Y. C. (2014). Oxygen isotopic distribution along the otolith growth axis by secondary ion mass spectrometry: Applications for studying ontogenetic change in the depth inhabited by deep-sea fishes. *Deep-Sea Research I*, *84*, 50–58. https://doi.org/10.1016/j.dsr.2013.10.006

Shiao, J. C., Wang, S. W., Yokawa, K., Ichinokawa, M., Takeuchi, Y., Chen, Y. G., & Shen, C. C. (2010). Natal origin of Pacific bluefin tuna *Thunnus orientalis* inferred from otolith oxygen isotope composition. *Marine Ecology Progress Series*, *420*, 207–219. https://doi.org/10.3354/meps08867

Shimizu, K., Ushikubo, T., Hamada, M., Itoh, S., Higashi, Y., Takahashi, E., & Ito, M. (2017). H_2O, CO_2, F, S, Cl, and P_2O_5 analyses of silicate glasses using SIMS: Report of volatile standard glasses. *Geochimica et Cosmochimica Acta*, *51*(4), 299–313. https://doi.org/10.2343/geochemj.2.0470

Shimose, T., & Ishihara, T. (2015). A manual for age determinationi of Pacific bluefin tuna *Thunnus orientalis*. *Bulletin of Fisheries Research Agency*, *40*, 1–11.

Shirai, K., Otake, T., Amano, Y., Kuroki, M., Ushikubo, T., Kita, N. T., Murayama, M., Tsukamoto, K., & Valley, J. W. (2018). Temperature and depth distribution of Japanese eel eggs estimated using otolith oxygen stable isotopes. *Geochimica et Cosmochimica Acta*, *236*, 373–383. https://doi.org/10.1016/j.gca.2018.03.006

Śliwiński, M. G., Kitajima, K., Kozdon, R., Spicuzza, M. J., Fournelle, J. H., Denny, A., & Valley, J. W. (2016). Secondary Ion Mass Spectrometry Bias on Isotope Ratios in Dolomite–Ankerite, Part I: $\delta^{18}O$ Matrix Effects. *Geostandards Geoanalytical Research*, *40*(2), 157–172. https://doi.org/10.1111/j.1751-908X.2015.00364.x

Śliwiński, M. G., Kitajima, K., Spicuzza, M. J., Orland, I. J., Ishida, A., Fournelle, J. H., & Valley, J. W. (2018). SIMS Bias on Isotope Ratios in Ca-Mg-Fe Carbonates (Part III): $\delta^{18}O$ and $\delta^{13}C$ Matrix Effects Along the Magnesite–Siderite Solid-Solution Series. *Geostandards Geoanalytical Research*, *42*(1), 49–76. https://doi.org/10.1111/ggr.12194

Storm-Suke, A., Dempson, J. B., Reist, J. D., & Power, M. (2007). A field-derived oxygen isotope fractionation equation for *Salvelinus* species. *Rapid Communications in Mass Spectrometry*, *21*(24), 4109–4116. https://doi.org/10.1002/rcm.3320

Suzuki, N., Tanabe, T., & Nohara, K. (2014). Annual fluctuation in Pacific bluefin tuna (*Thunnus orientalis*) larval catch from 2007 to 2010 in waters surrounding the Ryukyu Archipelago , Japan. *Bulletin of Fisheries Research Agency*, *38*, 87–99. Retrieved from http://ss.fra.affrc.go.jp/bulletin/bull/bull38/38-03-04.pdf

Tanaka, Y., Satoh, K., Iwahashi, M., & Yamada, H. (2006). Growth-dependent recruitment of Pacific bluefin tuna *Thunnus orientalis* in the northwestern Pacific Ocean. *Marine Ecology Progress Series*, *319*, 225–235. https://doi.org/10.3354/meps319225

Tanaka, Y., Mohri, M., & Yamada, H. (2007). Distribution, growth and hatch date of juvenile Pacific bluefin tuna *Thunnus orientalis* in the coastal area of the Sea of Japan. *Fisheries Science*, *73*, 534-542. https://doi.org/10.1111/j.1444-2906.2007.01365.x

Tanaka, S. (2011). Skip spawning and spawning frequency of Pacific bluefin tuna around Japan. *Report of the Pacific Bluefin Tuna Working Group Workshop (ISC/11/PBFWG)*. Retrieved from http://isc.fra.go.jp/pdf/ISC11/Annex_5_ISC11_PBFWG-1_FINAL.pdf

Tanaka, Y., Tawa, A., Ishihara, T., Sawai, E., Nakae, M., Masujima, M., & Kodama, T. (2019). Occurrence of Pacific bluefin tuna *Thunnus orientalis* larvae off the Pacific coast of Tohoku area, northeastern Japan: possibility of the discovery of the third spawning ground. *Fisheries*

Oceanography, *29*(1), 46–51. https://doi.org/10.1111/fog.12445

Tawa, A., Ishihara, T., Uematsu, Y., Ono, T., & Ohshimo, S. (2017). Evidence of westward transoceanic migration of Pacific bluefin tuna in the Sea of Japan based on stable isotope analysis. *Marine Biology*, *164*, 94. https://doi.org/10.1007/s00227-017-3127-8

The SwissSIMS. (n.d.). *Sample preparation for SIMS analysis. https://swisssims.com/sample-preparation/*

The University of Edinburgh, School of Geosciences. (2017). *Preparation of Indium Mounts for SIMS Analysis. https://www.ed.ac.uk/files/imports/fileManager/IndiumMountPrep.pdf*

Thorrold, S. R., Campana, S. E., Jones, C. M., & Swart, P. K. (1997). Factors determining $\delta^{13}C$ and $\delta^{18}O$ fractionation in aragonitic otoliths of marine fish. *Geochimica et Cosmochimica Acta*, *61*(14), 2909–2919. https://doi.org/10.1016/S0016-7037(97)00141-5

Ueyanagi, S. (1969). Observations on the distribution of tuna larvae in the Indo-Pacific Ocean with emphasis on the delineation of the spawning areas of albacore, *Thunnus alalunga*. *Bulletin Far Seas Fisheries Research Laboratory*, *2*, 177–256.

Uozato, R. (2011). Validity of $\delta^{18}O$ in otoliths of bluefin tuna *Thunnus orientalis* as an indicator for ambient environment. MSc dissertation, The University of Tokyo, Kashiwa, Chiba (in Japanese)

Valley, J. W., & Kita, N. T. (2009). *In Sity Oxygen Isotope Geochemistry by Ion Microprobe*. (M. Fayak, Ed.). Toronto: Mineralogical Association of Canada.

Von Leesen, G., Ninnemann, U. S., & Campana, S. E. (2020). Stable oxygen isotope reconstruction of temperature exposure of the Icelandic cod (*Gadus morhua*) stock over the last 100 years. *ICES Journal of Marine Science*, *77*(3), 942–952. https://doi.org/10.1093/icesjms/fsaa011

Weber, P. K., Bacon, C. R., Hutcheon, I. D., Ingram, B. L., & Wooden, J. L. (2005). Ion microprobe measurement of strontium isotopes in calcium carbonate with application to salmon otoliths. *Geochimica et Cosmochimica Acta*, *69*(5), 1225–1239. https://doi.org/10.1016/j.gca.2004.05.051

Weidel, B. C., Ushikubo, T., Carpenter, S. R., Kita, N. T., Cole, J. J., Kitchell, J. F., Pace, M. L., & Valley, J. W. (2008). Diary of a bluegill (*Lepomis macrochirus*): Daily $\delta^{13}C$ and $\delta^{18}O$ records in otoliths by ion microprobe. *Canadian Journal of Fisheries and Aquatic Sciences*, *29*(12), 1641–1645. https://doi.org/10.1139/F07-157

Willmes, M., Lewis, L. S., Davis, B. E., Loiselle, L., James, H. F., Denny, C., Baxter, R., Conrad, J. L., Fangue, N. A., Hung, T. C., Armstrong, R. A., Williams, I. S., Holden, P., & Hobbs, J. A. (2019). Calibrating temperature reconstructions from fish otolith oxygen isotope analysis for California's critically endangered Delta Smelt. *Rapid Communications in Mass Spectrometry*, *33*(14), 1207–1220. https://doi.org/10.1002/rcm.8464

Wurster, C. M., & Patterson, W. P. (2003). Metabolic rate of late Holocene freshwater fish: evidence from $\delta^{13}C$ of otoliths. *Paleobiology*, *29*(4), 492–505.

Wurster, C. M., Patterson, W. P., Stewart, D. J., Bowlby, J. N., & Stewart, T. J. (2005). Thermal histories, stress, and metabolic rates of chinook salmon (*Oncorhynchus tshawytscha*) in Lake Ontario: Evidence from intra-otolith stable isotope analyses. *Canadian Journal of Fisheries and Aquatic Sciences*, *62*(3), 700–713. https://doi.org/10.1139/f04-241

Wycech, J. B., Kelly, D. C., Kozdon, R., Orland, I. J., Spero, H. J., & Valley, J. W. (2018). Comparison of $\delta^{18}O$ analyses on individual planktic foraminifer (*Orbulina universa*) shells by SIMS and gas-source mass spectrometry. *Chemical Geology*, *483*(November 2017), 119–130. https://doi.org/10.1016/j.chemgeo.2018.02.028

Yabe, H., Ueyanagi, S., & Watanabe, H. (1966). Studies on the early life history of bluefin tuna *Thunnus thynnus* and on the larvae of the southern bluefin tuna *T. maccoyii*. *Report of Nankai Regional Fisheries Research Laboratory. 23*, 95–129.

Zazzo, A., Smith, G. R., Patterson, W. P., & Dufour, E. (2006). Life history reconstruction of modern and fossil sockeye salmon (*Oncorhynchus nerka*) by oxygen isotopic analysis of otoliths, vertebrae, and teeth: Implication for paleoenvironmental reconstructions. *Earth and Planetary Science Letters*, *249*(3–4), 200–215. https://doi.org/10.1016/j.epsl.2006.07.003